This page was intentionally left blank

Diagnostic Applications of Lasers

Copyright Information

About LASER-TEC

LASER-TEC is a not-for-profit National Center for Laser-Photonics and Fiber Optics Education. It is funded by the National Science Foundation to develop a sustainable pipeline of qualified laser and fiber optics technicians to meet the industry demand across the United States.

To learn more about LASER-TEC, visit www.laser-tec.org

About the Author of this Edition

Nathaniel Fried, Ph.D. is a Professor in the Department of Physics and Optical Science at the University of North Carolina at Charlotte. He also holds adjunct faculty positions in the urology departments at Johns Hopkins Medical School and Carolinas Medical Center. He completed his Ph.D. in Biomedical Engineering from Northwestern University (Evanston, IL) and a joint postdoctoral fellowship between the Johns Hopkins Applied Physics Laboratory (Laurel, MD) and the Biomedical Engineering Department at Johns Hopkins Medical School (Baltimore, MD). He has published over 200 journal articles and conference proceedings papers in the field of laser-tissue interactions, biomedical optics, and laser medicine. He currently teaches courses at UNC-Charlotte on Physics in Medicine and Biomedical Optics. His research interests include therapeutic and diagnostic applications of lasers in urology.

Table of Contents

Preface

About the LASER-TEC Laser and Fiber Optics Educational Series

This series was created for use in engineering technology programs such as electronics, photonics, laser-electro-optics, and related programs. This series of publications has three goals in mind:1) to create educational materials for areas of laser electro-optics technology in which no materials exist 2) work with industry to use, adapt and enhance available industry-created material, 3) make these materials available to technicians at no cost to them making education in these areas more accessible to everyone. The Laser and Fiber Optics Educational Series is available for free online at www.laser-tec.org.

About Diagnostic Applications of Lasers

Diagnostic Applications of Lasers was created to provide a fundamental background for technicians on the theory of optical imaging, microscopy, and spectroscopy, as well as other major imaging modalities in medicine, (e.g. ultrasound, nuclear imaging, x-rays, and computed tomography). There are numerous examples of successful optical diagnostic technologies, such as the pulsed oximeter for the measurement of blood oxygenation levels and optical coherence tomography for diagnosis of ophthalmic diseases. Promising emerging fields are also briefly covered, such as super-resolution microscopy and photoacoustic tomography.

To the Student

This book is written at the technician level and can be used in post-secondary electronics engineering technology, or related programs. Medical laser technology is used for minimally invasive surgical applications in a variety of medical fields. The book contains all the modern pedagogy, which includes the following sections: introduction-motivation, learning outcomes, self-test questions for each section, summary, glossary, bibliography, and rich colorful illustrations.

To the Instructor

This book is intended for use in a certificate or associate degree program in electronics engineering technology. This will not only update the course content but will provide the student with the latest skills that industry expects. A power point presentation and a test bank are available by sending a request using an official college email to info@laser-tec.org.

Acknowledgments

This text is based on work contributed by Dr. Nathaniel Fried in 2020, under the direction of Dr. Chrys Panayiotou, principal investigator of LASER-TEC. It is based on work done by Dr. Fred Seeber and Dr. Tom MacGregor, under the direction of Dan Hull, principal investigator of OP-TEC in 2008. The content of this module has been reviewed for technical accuracy and pedagogical integrity by industrial and academic reviewers listed below.

Senior Contributing Authors and Editors

2022 edition:
Author: Dr. Nathaniel M. Fried, University of North Carolina at Charlotte, Charlotte, NC
Editor: Dr. Chrysanthos A. Panayiotou, Indian River State College, Fort Pierce, FL

2008 edition:
Authors: Dr. Fred Seeber, Camden County College, Blackwood, NJ.
Dr. Tom MacGregor, Camden County College, Blackwood, NJ
Editor: Dr. Leno Pedrotti, CORD, Waco, TX

Diagnostic Applications of Lasers

Introduction

The use of light and optics is fundamental to the medical diagnosis of many diseases. For example, the current gold standard is a biopsy, the extraction of a small piece of tissue from the body, for processing, sectioning, and staining, to allow detailed observation using a standard light microscope by a pathologist. However, this form of diagnosis is limited in that the diagnosis cannot be made in situ (on location) or in real-time, and tissue processing artifacts can make analysis difficult and inaccurate as well.

Since the discovery of the laser in 1960, lasers and optical technologies in general have continually improved over time. The ultimate goal of medical diagnosis using optical imaging modalities is to be able to make a detailed and accurate medical diagnosis in situ and in real time. This module provides an overview of established imaging modalities (e.g. x-rays, computed tomography, single photon emission computed tomography, positron emission tomography, and ultrasound) as well as emerging imaging modalities (e.g. optical coherence tomography, optical transillumination, photon migration imaging, and photoacoustic tomography). The module also provides basic definitions for fundamental optical parameters (e.g. magnification, resolution, contrast, image depth,...etc) within the context of optical microscopy. Other, non-imaging diagnostic techniques, such as spectroscopy, are discussed as well.

This module and the companion module *Therapeutic Applications of Lasers* provide an overview of the uses of lasers in medical and surgical diagnostic and therapeutic applications.

Prerequisites

The student should be familiar with the following before attempting to complete this module.

1. High school mathematics through intermediate algebra and the basics of trigonometry
2. LASER-TEC Optics and Photonics Series Course 1, *Fundamentals of Light and Lasers*
3. LASER-TEC Optics and Photonics Series Course 2, *Elements of Photonics*

   Module 2-1: *Operational Characteristics of Lasers*

   Module 2-2: *Specific Laser Types*

   Module 2-3: *Optical Detectors and Human Vision*

Learning Outcomes

Upon completion of this module, the student should be able to do the following:

- Compare major imaging modalities (e.g. MRI, US, x-rays/CT, nuclear imaging-SPECT/PET, optical imaging, and microscopy for biopsy) in terms of resolution, image depth, source of contrast, and cost.
- Understand the principles and applications of optical and laser scanning microscopes including confocal microscopy.
- Describe the interaction of light with matter and describe image characteristics.
- Understand terms such as *magnification*, *resolution*, and *contrast*.
- Explain the principle of confocal laser scanning, multiphoton, and near field microscopes.

- Understand different types of spectroscopy including absorption spectroscopy, elastic scattering spectroscopy (Rayleigh scattering), inelastic scattering spectroscopy (Raman scattering), and fluorescence spectroscopy.
- Describe how x-ray and near-infrared transillumination works.
- Understand the concepts of light applications in optical coherence tomography, Doppler velocimetry, and medical tomography.
- Describe how ultrasound imaging works.
- Explain the basic concepts and applications of ballistic photon imaging, diffuse optical tomography, and photoacoustic imaging.

1. Introduction to Medical Imaging

Figure 1 plots major imaging modalities as a function of both their resolution and image depth. Notice that one can almost draw a diagonal line from the origin and bottom left to the top right, suggesting that there is a fundamental trade-off between image resolution and image depth (Table 1). Whole body imaging modalities such as CT (x-rays), MRI, and nuclear imaging (SPECT and PET) are limited by resolution on the millimeter to centimeter scale. Ultrasound and photoacoustic imaging modalities have resolutions and image depths that scale based on the frequency of the ultrasound transducer used. Optical coherence tomography and microscopy offer cellular and sub-cellular image resolution, but are limited to superficial imaging depths of less than 1-2 mm in opaque (non-transparent) tissues, primarily due to attenuation from multiple light scattering.

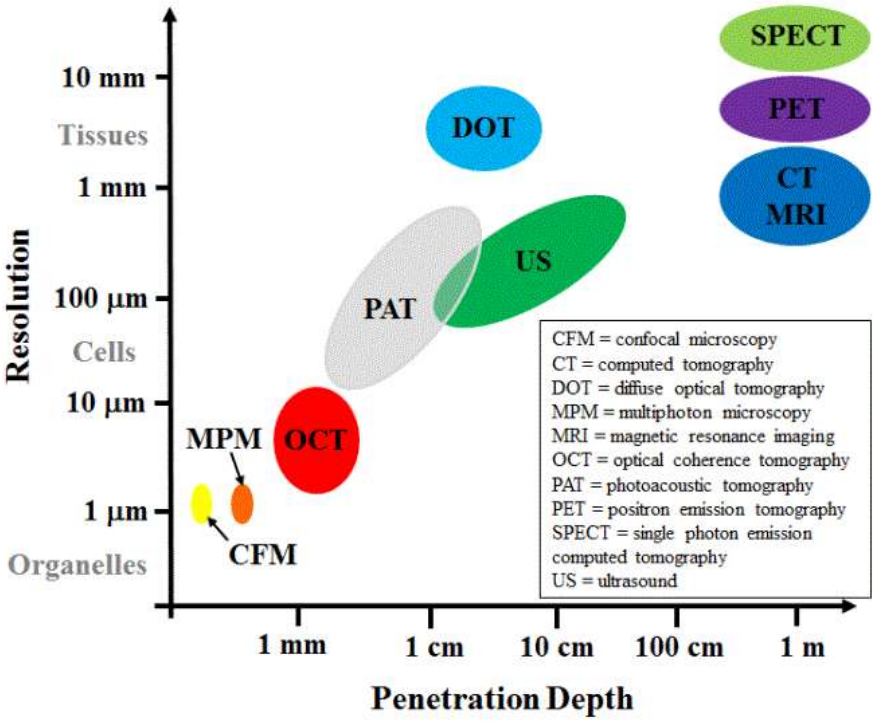

Figure 1. The trade-off between image resolution and image depth for standard imaging techniques.

Table 1. Specifications of Major Medical Imaging Modalities

Imaging Modality	Resolution	Image Depth	In Vivo (live use)?	Source of Contrast	Cost
Nuclear Imaging (PET/SPECT)	5-20 mm	Whole Body	Yes	Nuclear Isotope	$$$
Computed Tomography (CT/X-rays)	~ 1 mm	Whole Body	Yes	Attenuation	$$$
Magnetic Resonance Imaging (MRI)	~ 1 mm	Whole Body	Yes	Hydrogen Ion concentration	$$$$
Ultrasound (US)	100-500 μm	10-20 cm (Organs)	Yes	Acoustic Scattering	$$
Optical Coherence Tomography (OCT)	1-10 μm	2-3 mm	Yes	Light Absorption and Scattering	$$
Histology – Gold Standard (Optical biopsy + Microscope)	1 μm	5-10 μm Section	No	Histologic Stains	$

We will discuss many of these major imaging modalities in the following sections. As we do, note some of relative advantages and disadvantages of each imaging modality (Table 2).

Table 2. Comparison of Major Medical Imaging Modalities

Imaging Modality	Advantages	Disadvantages
Nuclear Imaging (PET/SPECT)	Good contrast; Functional imaging	Ionizing radiation; Poor resolution; Expensive
Computed Tomography (CT/X-rays)	Fast; Whole body image	Ionizing radiation; Poor soft tissue contrast
Magnetic Resonance Imaging (MRI)	Good soft tissue contrast; Functional imaging; Safe	Expensive; Slow imaging
Ultrasound (US)	Good resolution; Safe; Inexpensive	Image depth limited to organs; Imaging limited to contact mode
Optical Coherence Tomography (OCT)	Very good resolution; Non-contact imaging; Safe; Inexpensive	Superficial imaging depth limited by multiple light scattering
Histology – Gold Standard (Optical biopsy + Microscope)	Very good resolution; Inexpensive	Invasive; Not real-time imaging; Not in situ imaging

In particular, optical imaging techniques provide a number of useful characteristics. Advantages of optical imaging include:

- Already a diagnostic tool used for visual assessment and basis for minimally invasive surgery (e.g. microscopes and endoscopes). Vision is one of our five senses.
- Very good spatial resolution, on the order of the wavelength (λ) of the light (e.g. use of microscope to examine tissue biopsy is the current gold standard for diagnosis).
- Excellent temporal (time) resolution (e.g. to probe fast biochemical processes and time-resolved resolution).
- Convenient use of small, flexible, biocompatible, robust, and inexpensive fiber optic delivery systems. Most optical imaging is performed using visible or near-IR wavelengths, which can be delivered through standard silica optical fibers for minimally invasive surgery and diagnosis with access to internal surfaces of the body.
- Safe. Deeply penetrating visible and near-IR wavelengths provide non-ionizing radiation. No radiofrequency interference, so compatible with MRI systems as well.
- Low cost. Price comparable to ultrasound and much less than MRI, CT, PET, and SPECT.

Self-Test

1. Which of the following imaging modalities does not use ionizing radiation?
(a) CT (b) PET (c) US (d) SPECT

2. Which of the following imaging modalities is compact, portable, and inexpensive?
(a) MRI (b) US (c) CT (d) PET

3. What is currently considered the gold standard for diagnosis of diseases?
(a) X-rays (b) MRI (c) US (d) Biopsy

4. Which of the following imaging modalities does not provide functional imaging?
(a) MRI (b) PET (c) SPECT (d) They all provide functional imaging

5. Which of the following is a disadvantage of tissue biopsy?
(a) Invasive (b) Delayed diagnosis (c) No real time imaging (d) All of the above

6. What advantage does OCT have over other imaging modalities?
(a) Better resolution (b) Inexpensive (c) Compact and portable (d) All of the above

7. What major disadvantage does OCT have compared to other imaging modalities?
(a) Poor image depth (b) Slow image acquisition (c) Poor image resolution (d) All of the above

2. Principles of Microscopy

2.1 Introduction

In the biomedical field, optical microscopy is considered the gold standard for the diagnosis of diseases. For example, it is standard to remove a small piece of tissue from a suspicious region of the body (e.g. a potential tumor or abnormal mass) for inspection. This is called a *biopsy*. During a biopsy, the tissue sample is typically either frozen to provide a fast section for diagnosis, or instead placed in formalin (formaldehyde) to permanently fixate the connective tissue proteins. The water component of the tissue is then removed from the sample using progressively higher concentrations of alcohol baths, and then finally immersed in xylene, an optical clearing agent, to make the tissue more transparent. Then the tissue is embedded in wax, to provide a firm substrate for creating very thin sections (4-6 micrometers) with a very fine knife (microtome). The thin section is laid on a water bath to smooth out any wrinkles or artifacts, and then placed on a microscope slide for staining different cellular components. Finally, the stained thin tissue section is placed on a microscope slide, sealed with a cover slip, and placed under a standard optical transmission microscope, for observation and diagnosis by a trained doctor. This entire preparation method is commonly referred to as histology or histo-pathology, and the doctor is called a pathologist.

However, the main point to be noted here is that our current gold standard for diagnosis of diseases involves the use of high-resolution light microscopy (Figure 2). Therefore, it is important to have a fundamental understanding of how optical microscopes work.

The term *photo* relates to light. In this module we introduce techniques and instruments that use light sources such as compound microscopes, optical microscopes, and fluorescence imaging.

Lasers in conjunction with microscopes are used extensively in clinical diagnostics. We will study the working principles of microscopes such as magnification, resolution, and contrast. These are extremely important in the interpretation and analysis of medical imaging data. In this module, we also introduce the techniques of fluorescence imaging and its uses in medical diagnostics.

A microscope is an instrument for viewing objects that are too small to be seen by the unaided eye. The science of investigating microscopic objects using this instrument is called *microscopy*. The microscope is an important tool used in scientific research and has extensive applications in the practice of medicine.

A compound microscope consists of refractive glass or plastic lenses that focus light into the eye or some other type of optical detector. Microscopes can magnify an object to approximately 1500 times its normal size. This means that objects that are as close as 0.2 micrometers can be seen distinctly as two separate objects. Specialized techniques (e.g. scanning confocal microscopy and super-resolution imaging) may exceed this magnification.

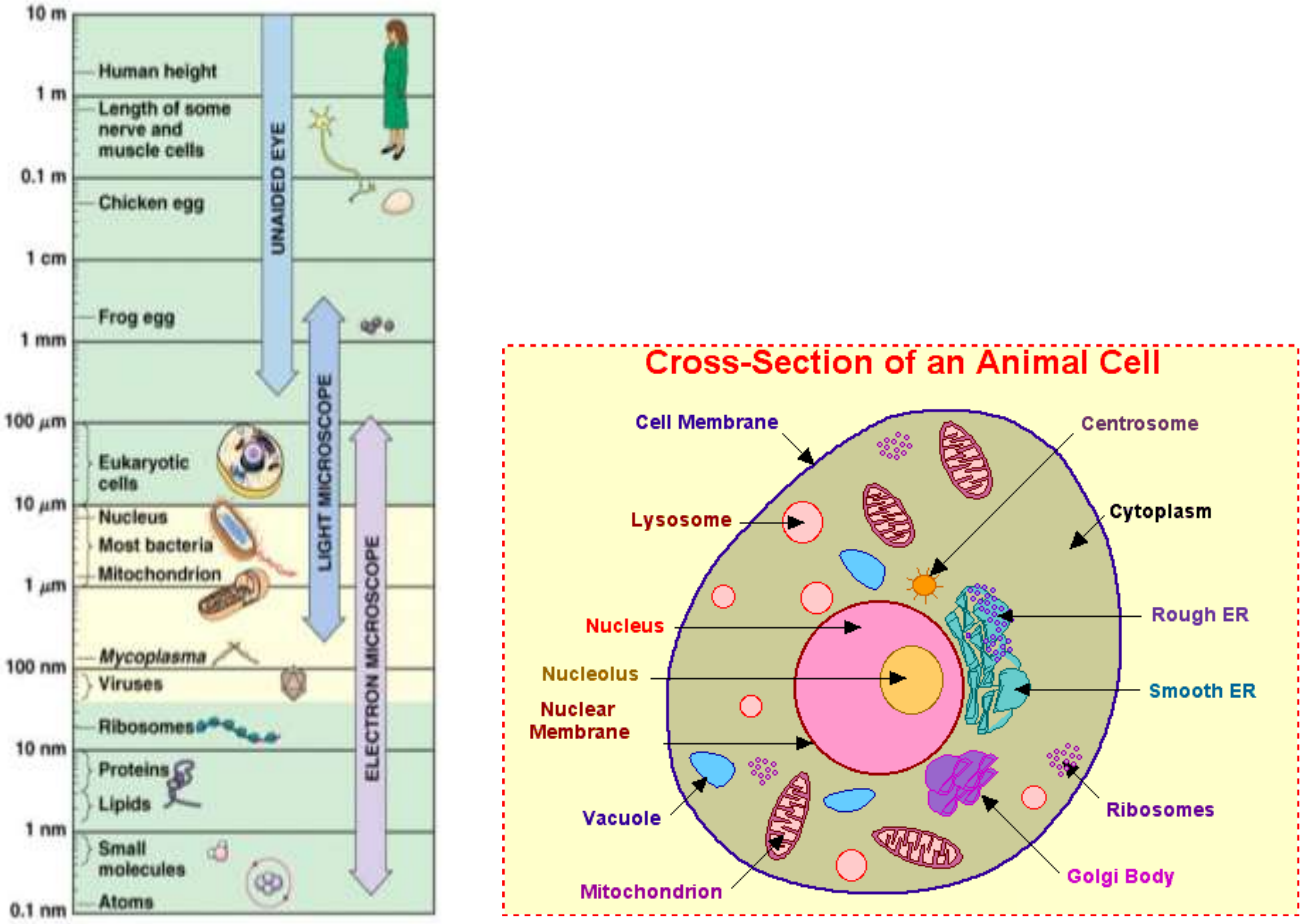

(a) (b)

Figure 2. (a) Scale of biological structures that can be resolved by the naked eye, light microscopes, and electron microscopes. Note that electron microscopy typically requires destroying the viability of a live sample due to the need to coat the surface with a gold layer. (b) Major sub-cellular structures of an animal cell. A single cell is typically on the order of tens of micrometers in diameter, the nucleus is 1-2 micrometers in diameter, and the cell membrane is about 10 nanometers thick.

2.2 Magnification

Magnification increases the dimension of the object. In a typical microscope, the magnification can range between 500 and 1500 times the actual size of the object. Another important consideration in magnification is “sensitivity.” For instance, the optical signal that comes from a fluorescence microscope can be extremely faint. Thus, any detector used with this microscope must be sensitive enough to

capture this signal and process it so that the magnified object can be viewed.

For a microscope, the angular magnification is given by:

$$(1) \qquad M = M_o * M_e$$

where M_o is the magnification of the objective lens and M_e the magnification of the eyepiece. Figure 3 illustrates how light rays emitted by the object, *O*, are processed by these two lenses to produce a magnified image, I_2.

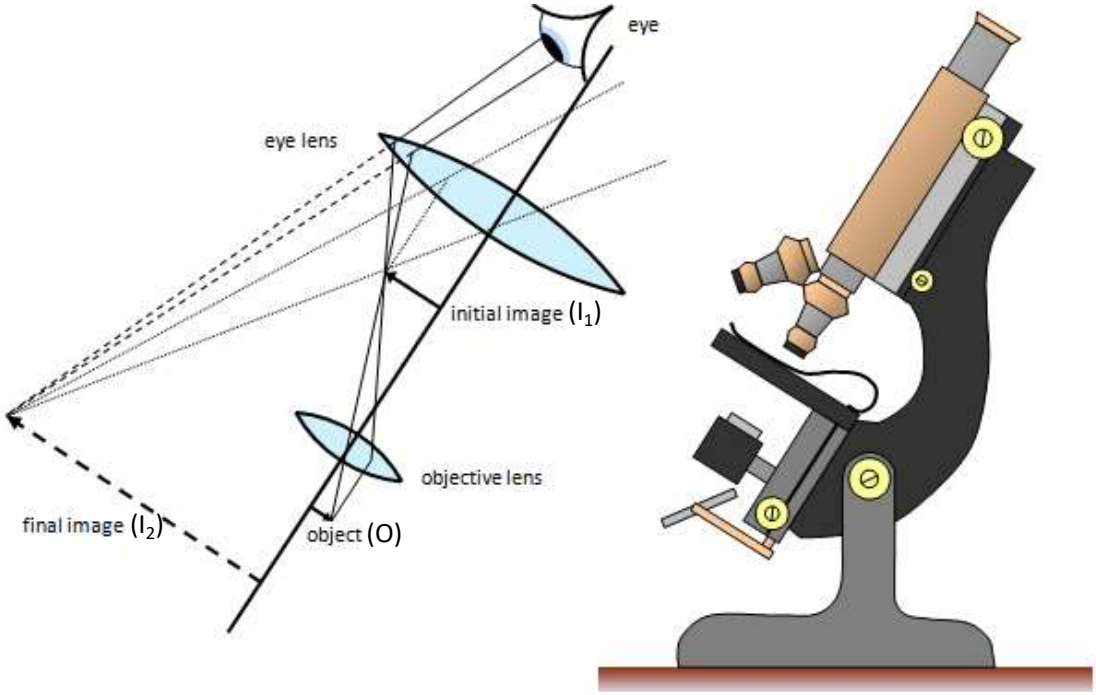

Figure 3. Magnification of a compound microscope.

2.3 Resolution

Resolution is the ability of an optical system (like a microscope) to distinguish, detect, and/or resolve the physical details of an object under observation. Several factors affect resolution. These include the *numerical aperture* of the system, an optical phenomenon called *diffraction,* and defects in lenses called *aberrations*.

Numerical aperture

The *numerical aperture* (*NA*) is a dimensionless quantity given by:

$$(2) \qquad NA = n\sin\theta$$

where n is the refractive index of the imaging medium and θ is the half angle of the maximum cone of light that can enter or exit the lens (see Figure 4).

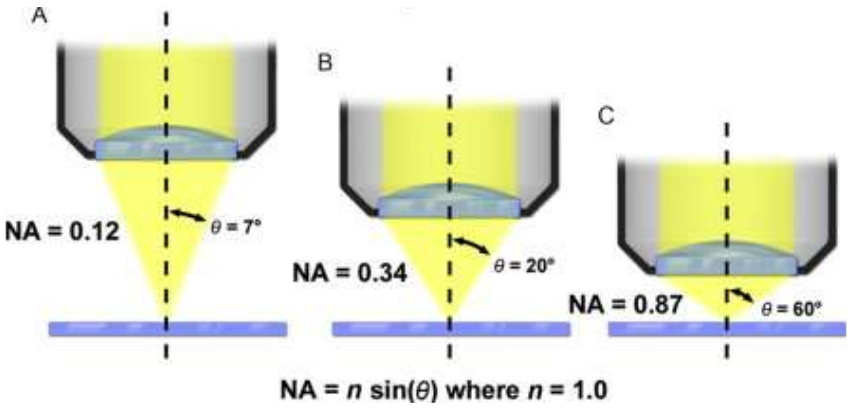

Figure 4. Microscope objective illustrating the light-gathering power of a lens and inverse relationship between numerical aperture and working distance for (a) NA = 0.12, (b) NA = 0.34, and (c) NA = 0.87.

Example 1
Calculate the numerical aperture of a microscope objective if n = 1.5 and θ = 38°.

Solution
NA = 1.5 sin (38°) = 0.923

The resolving power of a microscope is proportional to λ*NA*, where λ is the wavelength of the light being emitted by the object under observation. An objective lens with a larger NA will be able to visualize finer details than one with a smaller NA. Lenses with larger NA also collect more light and will generally provide a brighter image.

Diffraction

A more technical description of resolution was defined by Lord Rayleigh in 1879. He demonstrated that the resolution limit of a pure optical system is determined by diffraction. The phenomenon of *diffraction* occurs when light passes by the edge of an aperture. The light wave is disrupted by the edge and dispersed into a multitude of angles. This effect can be seen as a softening of the edges around a shadow. As light passes through a circular aperture diffraction generates a pattern called an Airy disc (Figure 5).

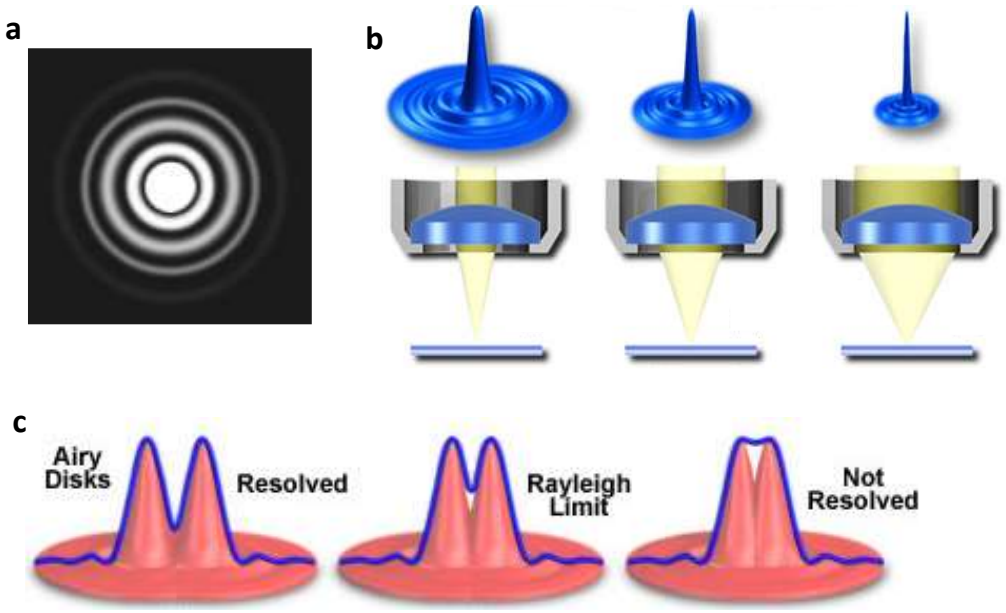

Figure 5. (a) Airy disc diffraction pattern produced by light passing through a circular aperture; (b) Relationship between numerical aperture and Airy disk size. As the numerical aperture increases, from left to right, the central maxima of the Airy disk gets smaller, and resolution improves; (c) Relationship between Airy disk separation and the Rayleigh criterion. When the central peaks of two objects overlap, they can no longer be resolved as separate objects.

Optical systems are typically limited by a circular aperture since lenses are fabricated based on spherical surfaces. Light passing through the system undergoes diffraction and produces an Airy pattern with a disc at the center called the Airy disc. No matter how high quality or large the lens becomes, the lens can never produce a single point of light. The image will always have the characteristic ring pattern seen in Figure 5. The Airy pattern dimensions are governed by the focal length and diameter of the limiting aperture of the system. All lenses can be expressed in terms of their *f*-number, F/#. The F/# is calculated by dividing the focal length, *f,* of a lens by the diameter of the limiting aperture of the system, *D*.

$$F/\# = f/D \quad (3)$$

The diameter of the Airy disc formed by a lens can be expressed as:

$$d = 2.44\,\lambda\,F/\# \quad (4)$$

where λ is the wavelength of the radiation coming from the object.

A *diffraction-limited* lens produces an Airy pattern. Taking into consideration Rayleigh's criterion and the fact that "real" lenses are not perfect, the diameter of the Airy disc gives a good approximation of the minimum distance two objects can be separated and still be resolved. The following equation defines this resolution:

$$\text{Resolution} = 2.44\,\lambda\,F/\# \quad (5)$$

Example 2
Given a lens with a focal length of 25.4 mm and a limiting aperture of 50 mm used at a wavelength of 632.8 nm, find the limiting resolution of this lens.

Solution

Resolution = 2.44 λ F/# = 2.44 λ (f/d) = (2.44) (632.8 x 10^{-9} m) (25.4 x 10^{-3} m / 50 x 10^{-3} m) = 0.784 x 10^{-6} m = 0.784 μm.

Because of imperfections in optical systems, most systems image points of light as small circular patterns with diameters larger than the diameter of the Airy disc. This circular pattern is referred to as the *blur spot*. The blur spot radius is always greater than the Airy disc radius.

Thus, Equation 5 calculates the theoretical minimum of resolution. In the real world the resolution is typically greater than this calculated value.

Example 3
If the visible spectrum range is from 400-700 nm, then consider the average wavelength for visible light in optical microscopy to be 550 nm (green light). Use the formula, Resolution = 1.22 λ / 2NA, where NA = nsinθ.

(a) Calculate the best theoretical resolution attainable.

(b) Placing a drop of oil (n = 1.52) between the sample and objective lens in a microscope improves resolution. Calculate the best theoretical resolution using an oil immersion lens.

(c) In practice, the angular aperture is limited to about θ = 72 degrees. For this value, calculate more practical values for each of the objectives above in air and oil.

Solution

(a) The best theoretical resolution is for n = 1 in air and θ = 90 degrees. In this case, NA = 1sin90° = 1. So,
Resolution = 0.61(550 nm) = 336 nm.

(b) Similarly, Resolution = [0.61(550 nm)] / 1.52 = 221 nm.

(c) For air, Resolution = [0.61(550 nm)] / sin72° = 353 nm.
For oil, Resolution = [0.61(550 nm)] / (1.52)(sin72°) = 232 nm

Aberrations

As just mentioned, a blur spot is the result of imperfections in the optical design called *aberrations*. These aberrations can be caused by simple misalignments in the optics or more complicated imperfections inherent in the surface shape of the lens. The major classes of aberrations are categorized as first-order and second-order. The first-order aberrations are the result of mechanical problems in the system: tilt and defocus. The second-order aberrations are caused by the surface shape of the lens and depend on where the object is located with respect to the optical axis of the system. The second-order aberrations, also called *Seidel aberrations,* are listed below in Table 3.

Table 3. Second-order Seidel Aberrations

Seidel Aberration	Effect
Spherical	On-axis rays are focused at a different point than off-axis rays
Coma	Rays through center of lens are focused to different plane than rays passing by lens edge
Astigmatism	Rays in vertical axis are focused to a different point than rays in horizontal axis

Distortion	Rays are non-uniformly distributed on the focal plane
Curvature	Rays are focused on a curved focal plane
Chromatic	Rays with different wavelengths are focused to different focal points

As aberration sources in an optical system increase, so does the diameter of the resulting blur-spot. As the size of the blur-spot increases, the performance of all imaging systems, including microscopes, degrade and their ability to resolve objects decrease.

2.4 Contrast

Contrast is defined as the relative difference in intensity or color between an object and its background. In the context of color, contrast is the ability to distinguish different colors from the background. Here, either the intensity or color must be different from that of the background. When samples are transparent, contrast-enhancing techniques are necessary to reveal details.

Since microscopes are widely used in medicine, selecting the proper one for a specific application is important. The concepts you have just studied are critical in making this selection. Magnification, resolution, and contrast are key parameters in matching a microscope to a specific medical procedure.

Self-Test

8. What is the smallest object that can be seen with the human eye unaided?
(a) Cell nucleus ~ 1 μm (b) Biological cell ~ 10 μm (c) Hair ~ 100 μm (d) Pen tip ~ 1 mm

9. What is the approximate minimum diffraction limited resolution (λ/2) of a light microscope?
(a) About 25 nm (b) About 250 nm (c) About 2.5 μm (d) About 25 μm

10. As the numerical aperture (NA) of the microscope is increased, the microscope objective working distance _____.
(a) Increases (b) Decreases (c) Stays the same (d) It depends on other parameters

11. The numerical aperture can be increased by _____.
(a) Increasing the refractive index n, by using an oil immersion objective
(b) Using a lens with a smaller acceptance angle
(c) Using a concave lens
(d) All of the above

3. Fluorescence Imaging Microscopy

3.1 Introduction

The microscopes studied in the last section used light that was reflected off an object or passed directly through it. In this section, we will study microscopes that use light that radiates from the object through fluorescence.

The absorption and subsequent re-radiation of light by organic and inorganic materials depends on either *fluorescence* or *phosphorescence*. The emission of light in fluorescence is simultaneous with the absorption of the excitation light. Once the excitation light is removed, fluorescence stops. Fluorescence lasts less than a microsecond. Contrast this to phosphorescence, where light continues to be emitted long after the excitation source is removed.

Fluorescence occurs when a *fluorophore* interacts with an incident photon. (A fluorophore is a component of a molecule that causes it to be fluorescent.) Absorption of the photon causes an electron in the

fluorophore to rise from its ground state to a higher energy level. When the electron returns to its ground level, a photon (fluorescence emission) is released with a wavelength that depends on the difference in energy between the ground state and the excited state of the electron. A given fluorophore may emit at a single wavelength or multiple wavelengths. Each fluorophore has a specific emission spectrum with the fluorescence emissions always having a longer wavelength than that of the excitation light.

Fluorescence emission depends on absorption and emission characteristics of the fluorophore, its concentration in the specimen, and optical path length of the specimen. Fluorescence produced (F) is given by the equation:

$$(6) \quad F = \sigma Q I$$

where σ is the molecular absorption cross-section, Q is the quantum yield, and I is the irradiance of the incident light. For example, for a type of fluorophore called *fluorescein,* the absorption cross-section is $\sigma = 3 \times 10^{-16}$ cm^2 per molecule, Q is about 0.99, and I = 3.37 x 10^{20} W/cm^2. This gives a value of 100,000 photons per second per molecule. The efficiency and resolution of the system are determined by how many of the emitted photons can be detected and how long the emission rate continues.

Care must be taken in using fluorophores. Fluorophores lose their ability to fluoresce when they are over-illuminated. This process is called *photobleaching*. Care must be taken to prevent photobleaching through the use of chemicals or by minimizing illumination. Illuminating a fluorophore can also cause phototoxicity, which can cause the death of cells being observed.

For the fluorescence to be observed, the contrast between the specimen and background should be high. This is achieved by labeling the area of interest with a fluorophore such as green fluorescent protein (GFP). A xenon or mercury arc discharge lamp is used as the exciting source.

Most fluorescence microscopes are *epifluorescent*, that is, they direct the excitatory light onto, rather than through, the specimen. Since most of the excitatory light is absorbed and not reflected, the light returning to the optical detector is primarily composed of the fluorescent emissions emanating from the specimen. Elimination of this reflected light allows the specimen to be more accurately analyzed. Another way to reduce unwanted light is through the use of filters.

Table 4 provides a list of some common *intrinsic fluorophores*, that is, biological molecules that fluoresce naturally due to their interaction with incident photons used for excitation.

Table 4. Common Intrinsic Fluorophores

Molecule	Excitation Wavelength (nm)	Fluorescence Wavelength (nm)
Tryptophan	280	300-350
Tyrosine	270	305
Flavin	380-490	520-560
Collagen	270-370	305-450
Melanin	340-400	360-560
NADH	340	450

Table 5 provides a list of some common extrinsic fluorophores, which are attached to molecules as labels to provide fluorescence.

Table 5. Common Extrinsic Fluorophores

Molecule	Excitation Wavelength (nm)	Fluorescence Wavelength (nm)
Dansyl chloride	350	520
Fluorescein	480	510
Rhodamine	600	615

Prodan	360	440
BIODIPY-FL	503	512
Texas Red	589	615

3.2 Fluorescence filters

Fluorescent imaging typically involves the collection of light from fluorophores or other fluorescent sources associated with the specimen under study. This light has a characteristic wavelength or band of wavelengths. The environment in which this imaging is done also contains similar and different wavelengths of light that come from other sources such as indoor lighting or sunlight. To ensure that fluorescent images are of the highest quality, environmental or background light must be eliminated or reduced during the imaging process. Fluorescent filters provide a means for significantly reducing background light.

There are several different types of fluorescent filters (Table 6). A laboratory in this module also provides a means for exploring how these enhance fluorescent images.

Table 6. Fluorescent filter types and functions

Filter Type	Function
Emission	Allow specific wavelengths to reach the detector
Long-pass	Allow all wavelengths to reach the detector
Band-pass	Allow only specific wavelengths to reach the detector
Dichroic	Allows a small bandwidth of wavelengths to reach the detector
Neutral density	Keeps certain bands of wavelengths, like UV or IR, from entering the detector

Another way to ensure that the maximum amount of light from a specimen is observed is to make certain that the light emanating from the specimen has a wavelength different from those of environmental or background sources. Some optical detectors can differentiate between wavelengths and only allow those from the specimen to be observed. One way to take advantage of this scheme is for a fluorophore to exhibit a *Stokes shift*.

3.3 Stokes shift

When a molecule or atom absorbs light, it enters an excited electronic state. The Stokes shift occurs because the molecule loses a small amount of the absorbed energy before re-emitting the rest of the energy as luminescence or fluorescence at wavelengths longer than those of the absorbed light. The amount of wavelength shift depends on the time between absorption and emission. Fluorophores with a large Stokes shift are available. Figure 6 demonstrates the Stokes shift.

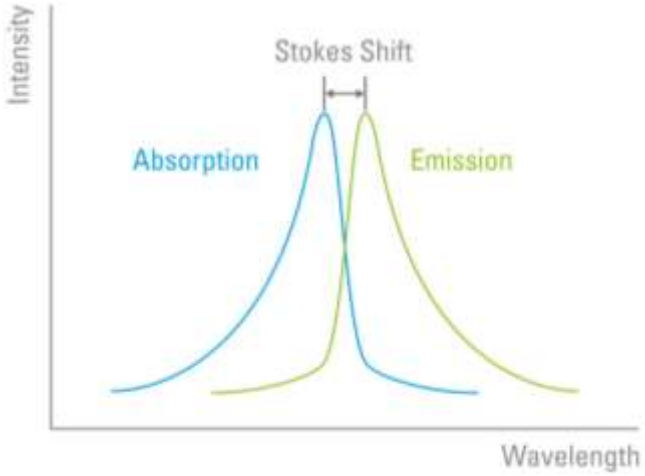

Figure 6. Schematic diagram showing Stokes shift.

While elimination of unwanted environmental or background light is important, it is equally important to collect as much of the specimen light as possible. *Image brightness* is a measure of how effectively a microscope performs this task.

3.4 Image brightness

Image brightness (a dimensionless quantity) is governed by the light-gathering power of the objective. Image brightness for epifluorescence, F_{epi}, is a function of numerical aperture and its magnification, and is defined by:

$$(7) \qquad F_{epi} = 10^4 \, NA^4 / M^2$$

Note that in fluorescence microscopy, brightness is inversely proportional to the objective magnification squared. Thus, for objective lenses of identical magnification, image brightness of both the illumination field and the fluorescence image increases dramatically with the objective lens numerical aperture. This is one of the primary reasons that manufacturers produce objectives designed with very high numerical apertures for fluorescence microscopy.

3.5 Applications

- Identify tissue changes caused by cardiovascular diseases
- Detect the presence of atherosclerotic changes
- Detect atherosclerotic coronary artery segments
- Image tumors
- Access coronary blood flow and perfusion of lung, heart, or kidney

3.6 Ratio Fluorescence Imaging

Fluorescence microscopy has long been used for qualitative characterization of subcellular distributions of proteins, lipids, nucleic acids, and ions. However, quantifying those distributions is complicated by a variety of optical, biological and physical factors. *Ratio fluorescence* imaging is a technique for determining these distributions.

The ratio fluorescence technique can be used to identify the location of intracellular free calcium in living cells, measure the concentration of intracellular ions and pH, and monitor the changes in intracellular ions. The ion-sensitive fluorescent probes, or dyes, are useful in identifying and measuring biologically significant, non-fluorescent substances.

Fluorescent dyes that are specific to calcium, sodium, magnesium, and potassium are available. When they bind to ions, their fluorescent properties are altered. Through quantitative study of the changes in fluorescent properties, the concentration of the ion being investigated can be measured. Calcium ions are the most widely studied because of the availability of a number of fluorescence probes or indicators, such as Indo-1, Fura-2, and SBR1, that can label the Ca^{2+} ion.

Fluorescence indicators are fluorophores that have specific medical applications. Several important processes, including signal transmission in nerve cells and muscle fiber concentration, are associated specifically with calcium ion activity. These Ca^{2+} indicators are chemicals in which the fluorescent emission is wavelength-shifted by binding to a particular metabolite, in this case, calcium ions. This is shown in Figure 7.

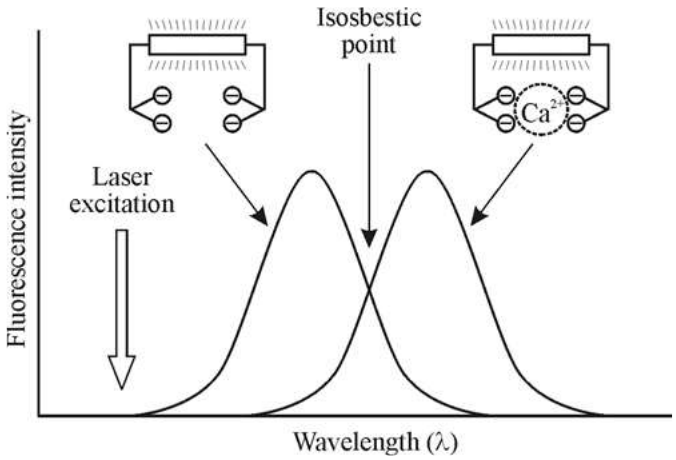

Figure 7. Presence of free calcium ions (Ca^{2+}) shifts the fluorescence-emission spectrum of a calcium indicator. At the isosbestic point, the total intensity remains constant, which is useful for ratioing or normalizing.

Changes in metabolic concentration and distribution can be studied by introducing one or more of these indicators into a living cell. A microscope is then used to acquire a sequence of fluorescent images at a single wavelength. Changes in calcium ion concentration show up as an increase or decrease in image intensity in different parts of the cell. In principle, absolute calcium concentrations and concentration differences can be obtained by calculating the ratio of image intensities at two different wavelengths. This requires use of an ultraviolet (UV) source.

The use of fluorescence ratios for measuring ionic concentrations such as intercellular Ca^{2+} and pH are well known. The same methodology can be used to observe and measure a variety of other cellular properties such as catabolism of internalized proteins, distribution of cellular lipids, trafficking of membrane proteins, and membrane fusion events. Using these methods, it is possible to follow biochemical and ionic changes, single organelles, or small regions of the cytoplasm in living cells. The range of applications is constantly expanding as new fluorescent probes are developed and new uses of existing probes are devised.

3.7 Immunofluorescence

Immunofluorescence involves the use of fluorescent dyes to label antibodies or antigens. Antibodies are Y-shaped proteins found in bodily fluids, including blood. The immune system uses antibodies to identify

and neutralize foreign objects such as viruses and bacteria. An antigen is a molecule that stimulates an immune response. Immunofluorescence is often used to visualize subcellular distributions of biomolecules.

Immunofluorescent-labeled tissues are examined using fluorescence microscopes or confocal microscopes. Ultraviolet light can be used to make the antigen-antibody combination visible. Antibody identification is performed on blood (serum) in the diagnosis of conditions such as myocarditis, syphilis, and toxoplasmosis, among others.

Fluorescent labeling is the process of covalently attaching a fluorophore to another molecule, for example, a protein or nucleic acid. This is typically accomplished using a reactive derivative of the fluorophore that selectively binds to a functional group contained in the target molecule. The most commonly labeled molecules are antibodies, which are then used as probes to detect particular targets. Fluorescent labels are detected by fluorescence microscopes or flow cytometers, which can identify targets embedded within cells.

Medical applications of this technique include the detection of the following:

- Colorado tick fever
- Focal segmental glomerulosclerosis
- Infectious mononucleosis (CMV)
- Infectious mononucleosis (EB)
- Lyme disease

3.8 Quantum dots as biological fluorescent markers

A *quantum dot* (QD) is a semiconductor nanostructure that restricts the movement of valence band holes, conduction band electrons, or excitons (bound pairs of conduction band electrons and valence band holes) in all three spatial directions. Quantum dots are composed of many, many atoms that behave like a huge single atom. Quantum dots have the ability to absorb incident light and emit light at a different wavelength.

The material used for the quantum dot must be a semiconductor, i.e., a material whose conductivity is somewhere between that of an insulator and a conductor. A key feature of quantum dots is that the color can be adjusted to any visible wavelength by changing the dot's size. Also called *nanocrystals,* these dots are typically 2–8 nm in diameter. Unlike molecular fluorophores, which typically have very narrow excitation spectra, semiconductor nanocrystals have the ability to absorb light over a broad spectral range. For this reason, it is possible to optically excite a broad spectrum of quantum dot "colors" using a laser. This allows simultaneous probing of several markers in biosensing and assay applications.

Quantum dots have three useful characteristics: (1) They can be designed to emit a specific frequency of light (specified by the user); (2) They can be configured to attach to any material through the use of an outside coating (3) Their fluorescent light radiates much brighter than traditional fluorescent labels. This makes them superior markers for biological experiments.

Quantum dots are useful in a variety of diagnostic applications. One example is the development of a fluorescent immunoassay using antibody-conjugated quantum dots. Several protein toxins have been successfully detected using this system. In another example, quantum dots embedded in polymer microbeads have been used for DNA hybridization studies.

Quantum dots are insoluble in water and are not easily attached to biological entities. When they are prepared, layers of organic ligands are coated onto their surfaces, making them hydrophobic. Various attempts have been made to make them water soluble by replacing these ligands with others that have hydrophilic ends, but this often degrades their optical properties. Polymer-coated quantum dots fulfill the promise of fluorescent semiconductor nanocrystals for both in-vivo and in-vitro studies. Figure 8 shows a

biocompatible conjugate QD.

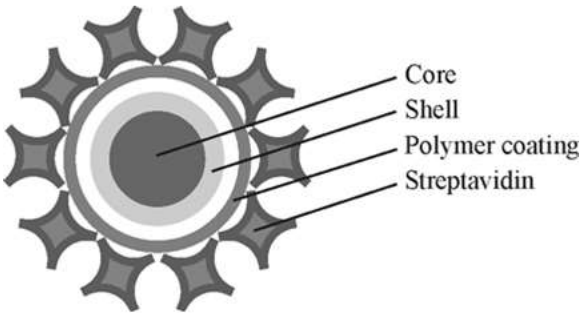

Figure 8. Schematic of a QD conjugate.

Diagnostic applications

- Antibodies labeled with quantum dots are a quick and extremely efficient way to detect bovine spongiform encephalopathy, otherwise known as mad cow disease.
- Allows bio-labeling of detection reagents for microscopy, flow cytometry, and immunoassay
- Creates a platform for multiplexed asseys such as proteomics, genotyping, and gene expression
- Allows live-cell and in-vivo imaging

3.9 Narrow band imaging (NBI)

Narrow band imaging (NBI) is an optical image enhancement technology that implements specific bandwidths to increase image contrast and visibility. NBI has been used for bladder cancer, colonic polyps, and Barrett's esophageal cancer detection during cystoscopy, utilizing two specific wavelength bands that are strongly absorbed by hemoglobin, blue light (440-460 nm) and green light (540-560 nm). NBI systems consist of narrow band filters in front of a white light source, or use of 415 nm and 540 nm light sources. Red light can be filtered out of the white light source via electronic control during the procedure. The 415 nm wavelength penetrates superficial layers of mucosa and is absorbed by capillary vessels, giving them a brownish hue, while the 540 nm wavelength penetrates more deeply, and is absorbed by blood vessels, giving them a blue appearance. The shorter wavelength is useful for detecting tumors, and the longer wavelength provides a better understanding of the vasculature of suspect lesions.

Self-Test

12. A major difference between fluorescence and phosphorescence is that fluorescence is _____.
(a) On shorter time scale (b) at different wavelengths (c) Is less intense (d) All of the above

13. The emission wavelength during fluorescence spectroscopy is ____than the absorption wavelength.
(a) Shorter (b) Same as (c) Longer (d) It depends
14. If a fluorophore experiences photobleaching then its fluorescence ____.
(a) Increases a lot (b) Is lost completely (c) Decreases slightly (d) Does not change

15. A quantum dot is approximately ___ in diameter.
(a) 5 nm (b) 50 nm (c) 500 nm (d) 5 μm

16. During narrow band imaging, ____ serves as a primary absorber of the excitation light.
(a) Water (b) Collagen (c) Hemoglobin (d) Elastin

4. Laser Scanning Microscopy (LSM)

4.1 Introduction

Laser radiation has advantages over ordinary light because of its high directionality and monochromatic nature. An additional advantage is the laser's ability to reach very small beam diameters and extremely high powers. A highly coherent laser beam can be focused down to its diffraction limit of only a few hundred nanometers.

Laser microscopy couples a laser to a microscope in a number of configurations and imaging modes. These configurations generate microscopic images by laser scanning. The laser beam on the sample excites fluorescence, which is collected. This fluorescence is then imaged onto a pinhole, which in a confocal geometry eliminates unwanted light that could obscure the desired image.

In this section the word *confocal* will be used several times. When *confocal* is used, it simply means that the focal point of the objective lens forms an image at the pinhole aperture. This is important because this optical arrangement increases the quality of the final image. Here is how: If the object we want to view is at the focal point of the objective lens, the vast majority of the fluorescence emanating from it will pass through the aperture. Light that comes from other objects, not located at the focal point, will be mostly blocked by the pinhole. Thus, the pinhole will pass through light from the object we want to examine and block light from objects of no interest.

LSM and *confocal LSM (CLSM)* can achieve high resolution and a high signal-to-noise ratio. They permit a wide range of quantitative measurements. These include topography mappings, extended depth focus, and 3D visualization. Some of the important LSM techniques include:

- Fluorescence microscopy, which involves the excitation of the sample at one wavelength and observation at another wavelength.
- Fluorescent micro-thermal imaging (FM), which uses the fluorescent emissions from a specimen to provide high-resolution spatial mappings of temperature distributions across surfaces.
- Excimer laser microscopy, which uses illumination in the deep UV to perform material removal functions through laser ablation.
- Multi-photon excitation spectroscopy, which uses two or more photons of different wavelengths to interact with a material and produce excitation spectra in a specified wavelength region.

4.2 Principle of operation

In CLSM, a fluorescent specimen is illuminated by a point laser source. The laser has a finite beam diameter that defines the spot size that scans the specimen. This spot size establishes the limit to how small a volume can be sampled on the specimen. When the laser scans the specimen, it illuminates a sample volume and causes it to fluoresce with a discrete intensity. The detector in the imagining system captures and stores the location of the volume and its fluorescent intensity. These data are then processed by a computer to create an image of the specimen.

The resolution of a CLSM is dependent on its beam size and ability to penetrate into the specimen. These two factors are called the *lateral resolution,* Δx, and *axial resolution,* Δz. The lateral resolution for CLSM and other confocal microscopes is given by:

$$\Delta x = 0.50\lambda / NA_{obj} \qquad (8)$$

The axial resolution defines the thickness of the probed slice or section thickness. It is evaluated by the

ratio of λ / NA^2. This ratio is used in Equation 9, which defines the axial resolution for CLSM and other confocal microscopes.

$$(9) \qquad \Delta z = 1.4n\lambda / NA_{obj}^2$$

In this equation, n is the refractive index of the objective lens immersion system.

Example 4
Calculate the axial resolution and the lateral resolution for a CLSM with an objective numerical aperture of 1.2 for an illuminating wavelength of 1.06 μm. Assume air as the medium between the objective and the spectrum.

Solution
Axial resolution = $\Delta z = 1.4n\lambda / NA_{obj}^2 = (1.4)\ (1)\ (1.06\ \mu m) / (1.2)^2 = 1.03\ \mu m$.
Lateral resolution = $\Delta x = 0.50\lambda / NA_{obj} = (0.50)\ (1.06\ \mu m) / 1.2 = 0.44\ \mu m$.

Figure 9 shows the schematic diagram of a CLSM. A laser provides the excitation light. An objective lens focuses the beam onto the specimen, where it excites fluorescence. The fluorescent light is collected by the objective lens and is directed onto the detector through a beam-splitter. The required range of the fluorescence spectrum is selected by an emission filter that also acts as a barrier blocking the excitation laser line. A pinhole is placed in front of the detector at the focal plane of the objective lens to suppress stray light, thus enhancing image contrast.

The detector is attached to a computer that builds up the image, one pixel at a time. A computer can generate a 3D image of the specimen by assembling a stack of 2D images from successive planes. Since a CLSM depends on fluorescent emissions, the specimen often must be treated with a fluorescent dye. However, the actual dye concentration must be very low so that it does not impact the biological effect being measured.

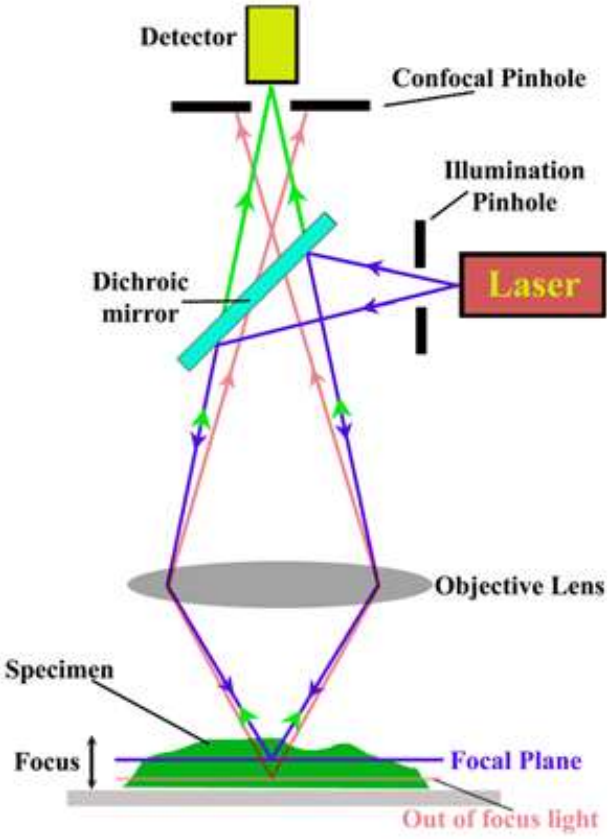

Figure 9. Schematic of a confocal laser scanning microscope (CLSM).

Table 7 summarizes the advantages and disadvantages of confocal microscopy as compared with conventional wide field light microscopy.

Table 7. Advantages and Disadvantages of Confocal Microscopy vs. Conventional Microscopy

Advantages	Disadvantages
Confocal aperture (pinhole) rejects out of focus light contributions to image	Confocal aperture reduces fluorescence signal level so a higher excitation power is needed, which in turn increases probability of photobleaching
Optical sectioning of tissue is possible	Most fluorophores are excited in the UV or blue spectrum, where light is highly attenuated in tissue
	Need for UV excitation light may result in degradation of the sample and limit time of observation

4.3 Applications

Confocal microscopy is clinically used in the following situations:

- In evaluating various eye diseases and, in particular, imaging *endothelial cells* of the cornea
- For localizing and identifying the presence of *filamentary fungal elements* in the *corneal stroma,* which are associated with keratomycosis
- For determining tumor margins in *basal cell carcinomas*, a type of skin cancer

- For identifying proliferative and inflammatory skin disorders
- For finding superficial tissue layers in the bladder and organs of living rats
- For generating freshly excised head and neck specimens
- For detecting drug delivery and distribution
- For determining the distribution of melanin and cell-to-cell interactions such as *diapedesis* and *apoptosis*

Self-Test

17. During confocal microscopy, a two-dimensional optical section is compiled consisting of _____.
(a) Depth scan (b) Two lateral dimensions (c) Depth and lateral dimensions (d) Angular scan

18. The axial resolution in confocal microscopy is dependent on which parameters?
(a) Wavelength (b) Numerical aperture (c) Refractive index (d) All of the above

19. The pinhole or aperture used in confocal microscopy serves the main purpose of ____
(a) Increasing intensity of light detected (b) Filtering wavelengths
(c) Rejecting out of focus light (d) All of the above

5. Multiphoton and Near-field Microscopy

5.1 Introduction

Two-photon excitation microscopy (also known as non-linear, multiphoton or two-photon laser scanning microscopy) is an alternative to confocal microscopy that provides a distinct advantage in 3D imaging. In particular, multiphoton excitation excels in imaging living cells such as brain slices, embryos, and whole organs.

As mentioned in the last section, the absorption of light can lead to photobleaching and phototoxicity. Two-photon excitation provides 3D optical sectioning without absorption. This technique offers greater depth of penetration than confocal microscopy.

5.2 Principle of multiphoton excitation

Two-photon excitation mechanism—Two-photon excitation takes place when a material simultaneously absorbs two photons. Since the energy of a photon is inversely proportional to its wavelength, the two absorbed photons must have a wavelength twice that required for one photon excitation. Figure 10 illustrates one- and two-photon excitation schemes in the UV and IR spectral regions.

From Figure 10(a) and (b), it can be seen that a fluorophore that normally absorbs UV radiation at about 350 nm can also be excited by two photons in the near IR region (about 700 nm), provided both reach the fluorophore at the same time (within an interval of about 10^{-18} sec). In order to produce a significant number of two-photon absorption events, the flux of photons causing this absorption event must be at least a million times that required to generate the same number of one-photon absorptions. This requires a high-powered laser.

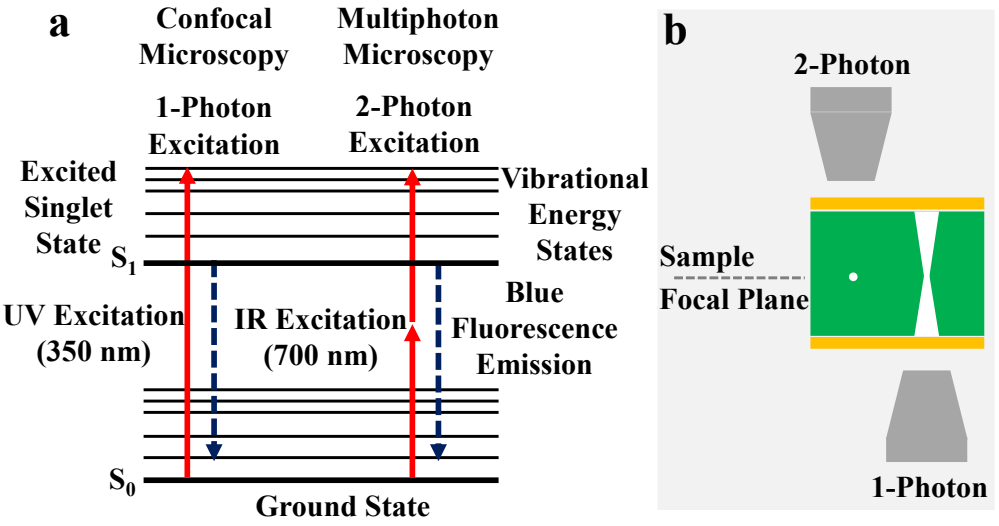

Figure 10. Schematic showing two-photon excitation mechanism as compared to a single photon excitation mechanism, such as with confocal microscopy.

5.3 Principle of operation

Two-photon absorption is accomplished with a laser scanner using a Ti-sapphire pulsed laser with a pulse repetition rate of about 80 MHz, a pulse width of 100 femtoseconds, and output radiation in the IR region. This type of laser generates the high-photon flux required for two-photon absorption.

The most commonly used fluorophores in two-photon absorption processes have excitation spectra in the 400-500 nm range, whereas the laser used to excite the fluorophores lies in the 700-1000 nm (near-infrared) range. If the fluorophore absorbs two infrared photons simultaneously, it will absorb enough energy to raise it to an excited state like that shown in Figure 10. The fluorophore will then return to a lower energy level by emitting a single photon whose wavelength will depend on the type of fluorophore used.

Two-photon fluorescence requires a highly focused laser beam. This focus is accomplished using lenses that focus the laser light on a small segment of the sample. The fluorescence emanating from this segment is collected by a highly sensitive detector. This fluorescence becomes the intensity of one sample point or pixel in the overall image of the specimen. By scanning the laser over the specimen, one can assemble a detailed image of the specimen's features from the individual pixels.

Problems encountered in two-photon microscopy include the following: (1) The two-photon absorption spectrum of a molecule may vary significantly from its one-photon counterpart, and wavelengths greater than 1400 nm may be significantly absorbed by the water in living tissue; (2) Short-pulsed lasers are generally expensive. (3) Special optics are required to withstand the intense pulses of the laser.

Table 8 summarizes advantages and disadvantages of two-photon microscopy versus confocal microscopy.

For a three-photon excitation mechanism, three photons interact simultaneously with the fluorophore to produce emission. The photon flux required for three-photon excitation is only ten-fold greater than the flux needed for two-photon absorption. Three-photon excitation can be used to extend the region of useful imaging into the deep UV. For example, 720-nm radiation can be used to excite a fluorophore that normally absorbs at 240 nm. As demonstrated in the last section, the shorter the wavelength of light, the greater the resolution. Examining the fluorescence from a fluorophore radiating in the UV region can offer more detailed imaging of the specimen.

Table 8. Advantages and Disadvantages of Two-Photon Microscopy vs. Confocal Microscopy

Advantages	Disadvantages
Utilizes a tightly focused beam, eliminating substantial out of focus fluorescence	Requires a very expensive ultra-short pulse laser
Enables optical sectioning without the need for a pinhole or confocal aperture	Use of special optical components needed to withstand intense light pulses
Greatly reduces photobleaching since excitation is quadratically dependent on intensity	
Near-infrared excitation wavelength penetrates much deeper in tissue due to less absorption and scattering	
Very good resolution; Non-contact imaging; Safe; Inexpensive	
Elimination of UV excitation light improves viability of cell samples	

5.4 Applications

Two-photon excitation reduces phototoxicity, increases tissue imaging depth, and can initiate localized photochemistry. Areas where two- and three-photon excitation microscopy are used include the following:

- Time lapse imaging of hamster embryo development
- In-situ imaging of human skin
- Imaging naturally occurring reduced pyridine nucleotides [NAD(P)H] as an indicator of cellular respiration
- Quantifying of glucose-stimulated insulin secretion (GSIS)
- Mapping the microcirculation in animal brain slices

5.5 Near-field scanning optical microscopy (NSOM)

In *near-field scanning optical microscopy* (NSOM), a subwavelength light source (i.e., the aperture diameter is smaller than the wavelength of light passing through it) is used as a scanning source. These sources are transmitted through a fiber optic cable that terminates in a tapered or conical tip. The specimen is attached to an X-Y positioner with nanometer movement. Using this positioner, the specimen is moved across the light source to illuminate the areas of interest. During this scan, the light source is kept at a constant distance from the specimen to ensure uniform sampling.

Illumination of a specimen with the “near-field” of a small light source enables construction of optical images with resolutions of about 50 micrometers. This technique is particularly useful in studying nondestructive, in-vitro, and in-vivo techniques for characterizing biological samples.

5.6 Light sheet fluorescence microscopy (LSFM)

A relatively new microscopy technique is called light sheet fluorescence microscopy (LSFM). During conventional microscopy, the biological sample is both illuminated and observed along the same optical axis, which provides good lateral resolution, but poor axial resolution, and produces significant background noise. Instead, LSFM uses a plane of illumination light perpendicular to the optical axis to observe slices of a sample. The light sheet illumination is kept fixed and the sample is moved up and down through the light sheet to capture different optical sections, that can then be assembled into a three dimensional image. The fluorescence only takes place in a thin section or layer of the sample. LSFM reduces contributions of out-of-focus light and improves the signal-to-noise ratio in the optical images. This technique can also acquire images at speeds several orders of magnitude faster than confocal

microscopy since LSFM scans the sample using a plane of light instead of a point.

5.7 Super-resolution microscopy

In recent years, multiple microscopy techniques have been developed which provide optical resolution that is better than the standard diffraction limited resolution of approximately $\lambda/2$. These techniques are classified within the field of super-resolution microscopy. Although much of the theory behind the operation of super-resolution microscopy is beyond this introductory text, it is important to at least be aware of this emerging field of microscopy. Many of these techniques are based on fluorescence imaging and provide resolution on the scale of tens of nanometers as compared to conventional microscopy techniques, which are limited to resolution on the order of hundreds of nanometers. As a result, super-resolution microscopy is sometimes referred to as nanoscopy instead of microscopy.

These techniques are non-linear, like multiphoton microscopy, and require application of several high-intensity, ultra-short pulse laser systems. One laser source is used to excite fluorophores in a sample to their fluorescent state, while a second laser is used for de-excitation of surrounding fluorophores by means of stimulated emission. Some common super-resolution techniques involving this method are called stimulated emission depletion (STED) microscopy and saturated structured illumination microscopy (SSIM). Another general approach to super-resolution microscopy is to make several localized fluorophores emit light on different time scales, so that these fluorophores can be separately resolvable in time. Some common super-resolution techniques involving this method are called photo activated localization microscopy (PALM) and stochastic optical reconstruction microscopy (STORM).

The main advantage of super-resolution microscopy is the improved optical resolution. For example, STED provides approximately 20 nanometer lateral and 40-50 nanometer axial resolution. The main disadvantages are similar to those of other nonlinear optical microscopy techniques (e.g. multiphoton microscopy), including the need to use very expensive, short-pulse, high intensity laser sources.

Self-Test

20. During two-photon microscopy, two photons in the ____ spectrum are used.
(a) UV (b) Green (c) Red (d) Infrared

21. Two-photon microscopy provides deeper imaging through tissue than confocal microscopy because photons in the ____ spectrum penetrate the deepest through tissue.
(a) UV (b) Green (c) Red (d) Infrared

22. What is an advantage of two-photon microscopy compared with confocal microscopy?
(a) Greater imaging depth (b) Less probability of photobleaching damage to tissue sample
(c) Elimination of UV light which can degrade sample lifetime (d) All of the above

23. What is a disadvantage of two-photon microscope compared with confocal microscopy?
(a) Poor image resolution (b) Poor sample lifetime (c) Cost of laser source (d) All of the above

24. Super-resolution microscopy techniques are capable of providing resolution on the order of ___, better than conventional microscopy.
(a) 20 nm (b) 200 nm (c) 2 μm (d) 20 μm

6. Spectroscopy

6.1 Absorption Spectroscopy

Perhaps the most successful example of optical diagnostics in medicine is the pulse oximeter, which uses absorption spectroscopy to non-invasively measure blood oxygen levels. The clip that is put on a finger or ear lobe in the hospital is a pulse oximeter. The pulse oximeter measures the percent of oxygenated blood, and is typically used for diagnosis in patients who are hypoxic (deprived of oxygen) before they become clinically cyanosed (where their skin turns blue due to a lack of oxygen).

Principle of Operation – Two light-emitting diodes (LEDs) transmit light, one at a red wavelength (e.g. 660 nm), that is more strongly absorbed by deoxygenated hemoglobin, and the other in the infrared (e.g. 920 nm) that is more strongly absorbed by oxygenated hemoglobin (Figure 11). A photodiode measures the intensity at each wavelength, and then a ratio is calculated for the percent hemoglobin that is saturated (SaO_2) given by:

$$(10) \qquad SaO_2 = [HbO_2] / [HbO_2 + Hb]$$

Under normal physiological conditions, arterial blood is 97% saturated, while venous blood is 75% saturated. Note that wavelengths in the red and infrared spectrum are also chosen because they penetrate the deepest through soft tissues. Also, note that because a ratio is calculated and not an absolute measurement, the variable tissue thickness (e.g. in the finger or ear) among different patients does not affect the measurement. The variable path lengths that the photons travel among different patients is not a factor.

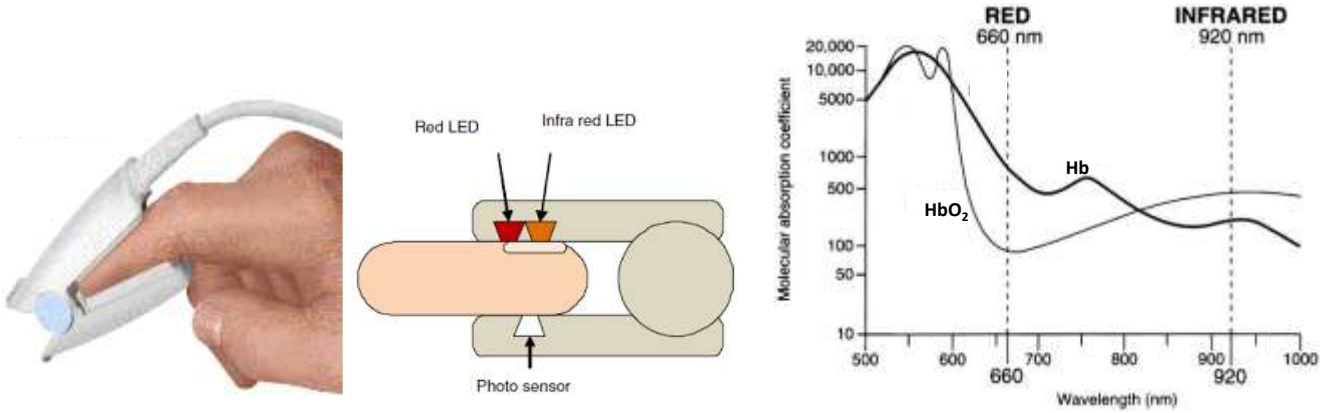

(a) (b) (c)

Figure 11. (a) Photograph of pulse oximeter clip. (b) Diagram showing emission by red and near-infrared LEDs and collection of light by a photodiode, to be sent to a computer processor. (c) Absorption spectrum of oxygenated hemoglobin (HbO_2) and deoxygenated hemoglobin (Hb).

Other applications of absorption spectroscopy:

It is interesting to note that Dual Emission X-ray Absorptiometry (DEXA) uses a similar principle to that of the pulse oximeter. In DEXA, two different x-ray energies are transmitted along the same path through a patient's soft tissues and bones. The ratio of absorption determines a patient's bone mineral density (BMD), given known tissue densities and mass attenuation coefficients. DEXA is used for diagnosis in

patients suffering from low BMD, known as osteopenia, or extremely low BMD, known as osteoporosis. Loss of bone mineral density in postmenopausal women is of specific concern. Hip fractures due to osteoporosis are a leading cause of morbidity and death in elderly women. The noninvasive technique of DEXA eliminates use of painful bone biopsies, and improves on the poor sensitivity of x-ray film in detecting slight changes in bone density.

6.2 Light Scattering Spectroscopy

Light scattering spectroscopy (LSS) is an optical technique for measuring the power spectral density of surface cellular structures and morphology. It permits in-vivo, non-invasive detection of structures in biological tissues at the intercellular level. LSS can provide quantitative measurements of parameters in real time without requiring tissue removal. This technique is used in the early detection of colon cancer.

The angular and wavelength distributions of light scattered by a cell nucleus depend on its size and refractive index. Thus, if light, directly back scattered from nuclei, is observed, the size and refractive index of these nuclei can be obtained from the spectral variations. However, for biological samples, the single scattering events can be masked. The light scattered back from a tissue specimen consists of two components - one due to a single-scattering event, and the other due to diffuse background light. In order to study a single-scattering event, the scattered light must be distinguished from the diffusive background.

Polarized light provides a means for distinguishing scattered light from background light. This is based on the fact that linearly polarized light incident on a turbid medium such as biological tissue loses its polarization as it traverses the medium and undergoes multiple scattering events. However, light that undergoes just a single scattering event will retain its polarization. When the polarized light (single scattered) and unpolarized light (multiple scatters) reach the optical detector of the LSS, their differences in polarization will allow them to be separated. Thus the single-scattered light spectrum that contains the information needed can be analyzed without the corrupting influence of the unpolarized light. This analysis can yield the size distribution of nuclei, their population density, and their refractive index.

In LSS, the light source is an arc lamp. Light is collimated by an achromatic lens. A broad-band polarizer, a narrow-band wavelength-selecting filter, beam splitter, and mirror combination are used. The spatial distribution of light emerging from the tissue surface is imaged onto an optical detector called a charged couple device (CCD) (Figure 12).

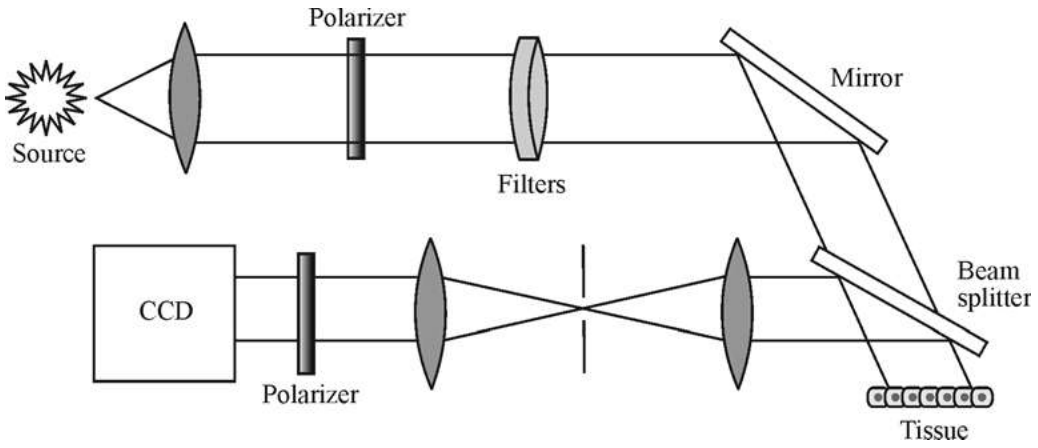

Figure 12. Schematic of a light scattering spectroscope.

Some applications of light scattering spectroscopy include:

- LSS imaging can be used to detect precancerous lesions in optically accessible organs such as the colon, cervix, and oral cavity.
- LSS-based imaging provides quantitative images of increased chromatic content of cells or tissues.
- LSS can provide early detection of cervical neoplasia in-vivo.
- LSS used in conjunction with fluorescence and reflectance spectroscopy can characterize plaque.

6.3 Raman spectroscopy

Raman spectroscopy is used to study rotational, vibrational, and other low-frequency modes in molecular systems. It depends on the inelastic scattering of photons by molecules that cause a frequency shift and, consequently, an energy shift of the photon (Figure 13). This shift provides information about the system.

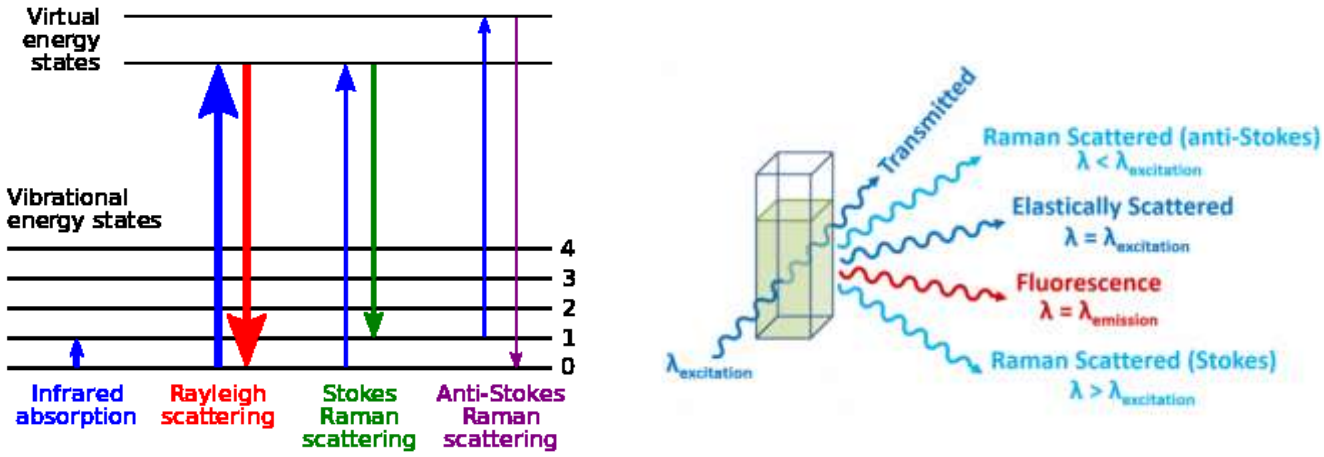

(a) (b)

Figure 13. (a) Energy states diagram, showing the difference between elastic scattering of photons, in which (b) the excitation and emission wavelengths are the same (e.g. Raleigh scattering) versus inelastic scattering of photons, in which the excitation and emission wavelengths are different (e.g. Raman scattering).

Raman microscopy generates very high spatial resolutions. This is because the objective lenses of the microscope focus the laser beam to a very small diameter, creating high photon fluxes. These photons cause Raman spectra to be generated in very small regions of the sample. Raman spectra contain information for measuring the properties of cells, proteins, organs, and erythrocytes and for studying biological samples such as DNA, peptides, and protein.

Raman microscopy is used extensively in monitoring blood gases under anesthetic conditions and observing skin cancers and other skin diseases. It is a noninvasive, nondestructive technique. It can be used to differentiate between subtle changes in tissue and to identify bio- terrorism agents such as anthrax. Determining chemical concentrations in biofluids, identifying teeth bacteria, and studying individual immune cells are other areas in where Raman microscopy is used.

Self-Test

25. Hemoglobin strongly absorbs light in the ____ spectrum.
(a) UV (b) Blue (c) Green (d) All of the above

26. A pulse oximeter uses the ratio of absorption at two wavelengths of light in ___ and ___ spectrum for oxyhemoglobin and deoxyhemoglobin, to measure blood oxygenation levels.
(a) UV and IR (b) Red and IR (c) UV and Visible (d) Green and Red

27. The pulse oximeter measurement of blood oxygenation is not dependent on the thickness of the patient's ear or finger because _____.
(a) No light is absorbed by the tissue (b) All the light is reflected by the tissue surface
(c) Ratio divides out path length of light (d) All of the above

28. Light is most strongly scattered by ___.
(a) Tissue structures that are the same size as the light (e.g. cell nuclei for visible and IR light)
(b) Interfaces between tissues that have very different refractive index values (e.g. Fresnel reflection)
(c) Tissue that has a high density of scatterers (e.g. melanin particles in skin)
(d) All of the above

29. Which of the following spectroscopy techniques uses elastic scattering of photons?
(a) Rayleigh scattering (b) Stokes Raman scattering
(c) Anti-Stokes Raman scattering (d) All of the above

30. A major disadvantage of using Raman spectroscopy in biomedical applications is the ___.
(a) Weak signal (b) Poor resolution (c) Expensive system (d) All of the above

7. Transillumination

7.1 X-ray transillumination

X-ray transillumination is commonly used in medicine for deep imaging and high contrast between tissues of different densities, such as soft and hard tissues (e.g. in dentistry and orthopedics) as well as locating small tumors (e.g. mammography). X-ray energies of 10-150 keV are typically used for medical imaging (where 1 eV = 1.6 x 10^{-19} J). The attenuation coefficient, μ, for x-rays traveling through tissues is dependent on both the tissue density, ρ, and the mass attenuation coefficient, μ_m, (which in turn is dependent on the chemical composition of the tissue in the form of the atomic number, Z, as well as the energy level of the x-rays). The equation for x-ray attenuation is given by:

$$\mu = \rho \, \mu_m \qquad (11)$$

The density is relatively constant for a given tissue. However, the mass attenuation coefficient increases inversely as the x-ray energy used decreases. The penetration depth of the x-rays is simply given by the inverse of the attenuation coefficient, or $1 / \mu$. Therefore, high energy x-rays travel deeper through tissue than low energy x-rays (Figure 14a).

The change in intensity, I, of the x-rays as they travel through tissue simply follows Beer's Law of exponential decay, similarly to optical radiation, but with a different attenuation coefficient.

$$I = I_0 \exp(-\mu x) \qquad (12)$$

where x is the depth in the tissue.

Example 5
In medical imaging procedures, lead aprons shield the body from exposure to ionizing radiation such as x-rays. Consider a lead apron with a thickness of 0.5 mm. What fraction of 140 KeV x-rays will be transmitted through the lead apron? Assume a mass attenuation coefficient of $\mu_m = 2.0\ cm^2/g$ and a density for lead of $\rho = 11.3\ g/cm^3$.

Solution
First, calculate the attenuation coefficient. $\mu = \rho\ \mu_m = (11.3\ g/cm^3)\ (2.0\ cm^2/g) = 22.6\ cm^{-1}$.
Now, use Beer's Law to calculate the collimated transmission (I/I_0).
Transmission = $I/I_0 = \exp(-\mu x) = \exp[-(22.6\ cm^{-1})\ (0.05\ cm)] = \exp(-1.13) = 0.32 = 32\%$

X-ray images are formed by different attenuations of the x-ray beam in the tissues. Objects with high attenuation produce shadows. There are several fundamental trade-offs in x-ray medical imaging. High energy x-rays penetrate deeper in tissues and hence experience less attenuation due to absorption and scattering of x-ray photons. The patient is therefore exposed to less radiation. However, only tissues which have high physical contrast can be imaged, due to differences in tissue densities. For example, chest and dental x-rays use relatively high x-ray energy settings because the natural difference in densities between the soft tissues and hard tissues (e.g. gums and teeth in dentistry, or rib bones and lungs in chest x-rays) are sufficient to produce a high contrast image. Conversely, x-ray mammography for the breast, which has inherently low physical contrast, requires the use of low-energy x-rays, which are more strongly attenuated to produce more contrast between normal soft fatty tissue and a breast tumor, for example. This use of low-energy x-rays comes at the expense of a higher dose of ionizing radiation to the patient and the need to compress the breast so the lower energy x-ray photons can penetrate sufficiently deep for imaging. The equation for image contrast is given by:

$$(13) \qquad C = (I_1 - I_2) / I_1$$

If we substitute the individual terms for I_1 and I_2 from Beer's Law, we can re-write the equation for contrast in terms of the attenuation coefficients and tissue thickness as:

$$(14) \qquad C = 1 - \exp[-(\mu_2 - \mu_1)x_2]$$

These variables are more clearly defined for a tissue (e.g. a tumor embedded in an organ) by Figure 14b.

Example 6
X-ray mammography is often used to detect small, micro-calcifications that are associated with the development of tumors in the breast. A contrast greater than 1% is typically sufficient for detection, Using Equation 14 above, calculate the contrast between a 100 μm micro-calcification ($\mu_1 = 0.4\ cm^{-1}$) and healthy tissue ($\mu_2 = 3.5\ cm^{-1}$) in the breast, for an x-ray energy of 25 KeV. Can the micro-calcification be detected. (3 pts)

Solution
$C = 1 - \exp[-(\mu_2 - \mu_1)x_2] = 1 - \exp[-(3.5 - 0.4)\ cm^{-1}\ (0.01\ cm)] = 1 - \exp[-(0.031] = 1 - 0.97 = 0.03 = 3\%$.
Yes, the micro-calcification can barely be detected using 25 KeV x-rays.

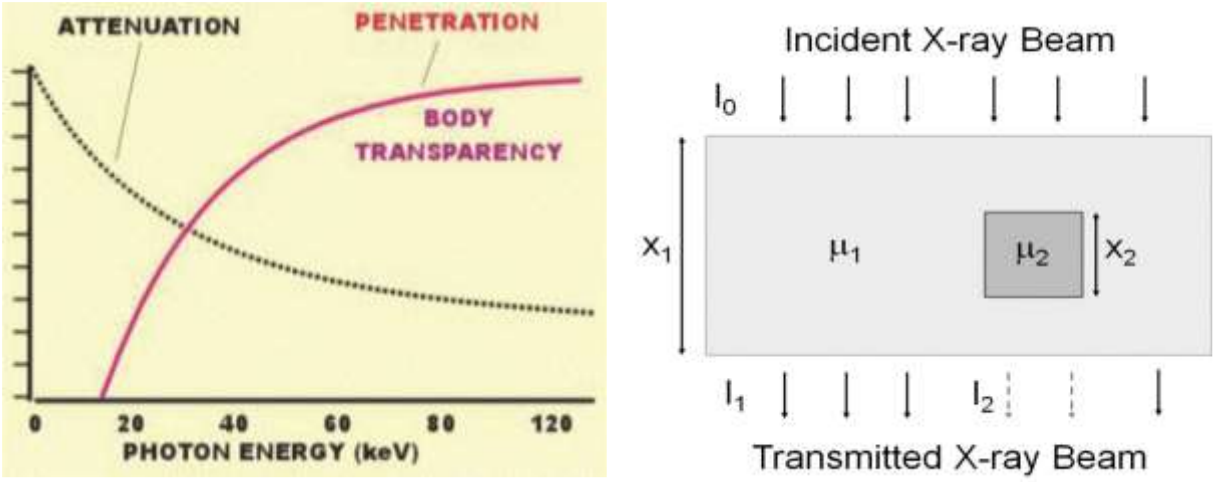

(a) (b)

Figure 14. (a) Trade-off between x-ray attenuation and penetration depth as a function of x-ray energy. (b) Diagram showing source of contrast due to attenuation coefficient and size of object during x-ray imaging.

7.2 Near-infrared transillumination

An inherent limitation of x-ray imaging is that x-rays are ionizing radiation, and the dose to the patient needs to be carefully monitored and limited due to safety reasons and the risk of cancer. Unlike x-rays, near-infrared light can be used for transillumination imaging of small tissue structures without exposing the patient to ionizing radiation (Figure 15).

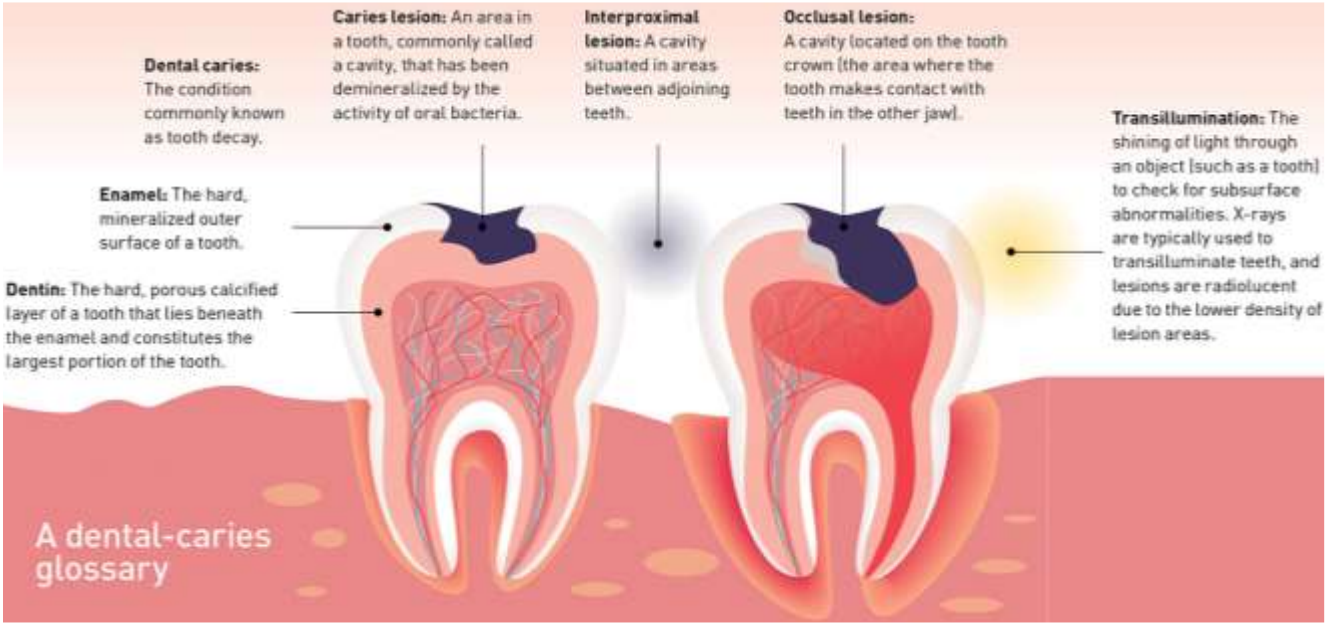

Figure 15. Anatomy of a tooth showing different locations of tooth decay and the potential of optical near-infrared transillumination to provide a safe, high-contrast alternative to imaging with ionizing x-ray radiation for early detection of tooth decay.

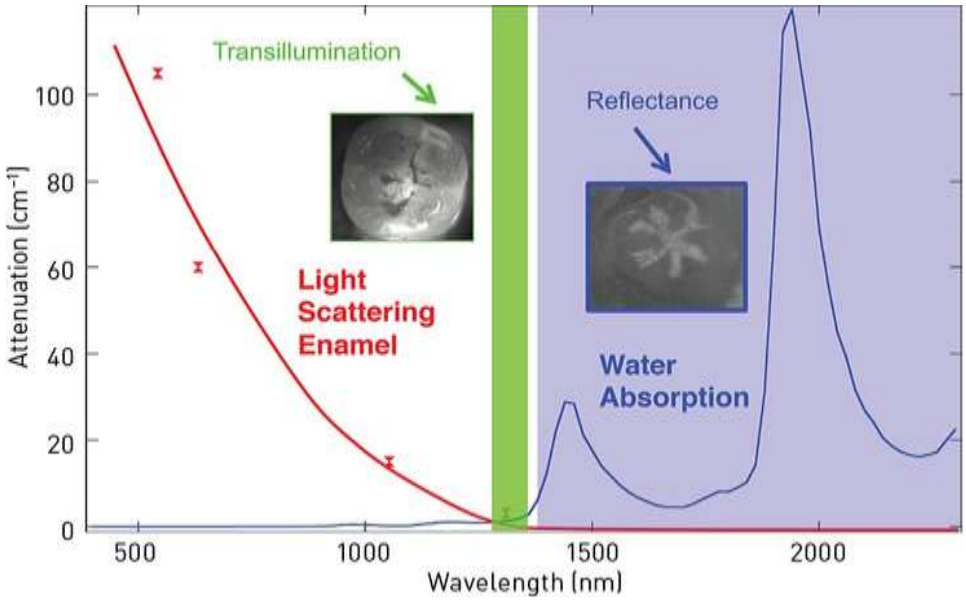

Figure 16. Light attenuation in dental enamel due to scattering decreases significantly in the near-IR spectrum, and water absorption peaks may also contribute to contrast in images in reflectance mode as well.

For example, near-IR transillumination can be used in dentistry to detect tooth decay. The decayed tissue produces a high amount of light scattering, which in turn produces higher light attenuation, as a source of contrast compared to the healthy dental tissue. Interestingly, dental enamel also has significantly lower light scattering in the near-infrared than the visible, so the dental enamel layer is translucent, and the dental enamel junction a few millimeters below the tooth surface can be imaged as well (Figure 16). Since dental decay usually originates in those difficult to reach locations such as pits and fissures along the tooth's surface, where fluoride from brushing cannot reach, optical techniques for early detection of dental caries appear quite promising.

Self-Test

31. The attenuation coefficient for x-rays is dependent of which of the following parameters?
(a) Tissue density (b) Tissue chemical composition (c) X-ray energy (d) All of the above

32. If the X-ray energy is increased, then imaging depth ____.
(a) Decreases (b) Increases (c) Stays the same (d) Insufficient information

33. X-ray mammography for breast cancer imaging uses low energy x-rays that provide _____.
(a) Less expensive imaging (b) Better contrast (c) Better resolution (d) Deeper imaging

34. Dental and chest x-ray imaging use high energy x-rays because ____.
(a) Better resolution (b) Faster imaging (c) Physical contrast is sufficient (d) All of the above

35. A major advantage of near-infrared transillumination compared with x-ray imaging is ____
(a) Safety - no ionizing radiation (b) Penetration depth (c) Speed (d) All of the above

8. Medical Tomography

8.1 Introduction

Tomography is a technique used to show a single plane, or slice, of an object. There are several forms of tomography. Three of the most widely used diagnostic techniques are discussed below.

8.2 Computed tomography (CT)

Computed tomography is an imaging method that uses X-rays to create cross-sectional, 2D images of the body. Images are acquired by rapid rotation of an X-ray tube 360° around the patient. The transmitted radiation is then measured by a ring of detectors surrounding the patient. The final image is generated from a reconstruction of multiple X-ray projections.

Early CT scanners acquired images one slice at a time (sequential scanning). More modern CT scanners use a spiral CT in which the X-ray tube rotates continuously in one direction while the table on which the patient is lying is moved through the X-ray beam. The transmitted radiation takes the form of a helix. Instead of being acquired one slice at a time, information is acquired as a continuous volume of slices.

Some CT scanners have multi-slice or multi-detector capabilities. They employ the spiral CT technique but incorporate multiple rows of detector rings. These machines can acquire multiple slices per tube rotation. This increases the area of the patient covered for a given time of X-ray exposure. Figure 17 shows a diagram of the CT scanning system and a normal CT scan of the head.

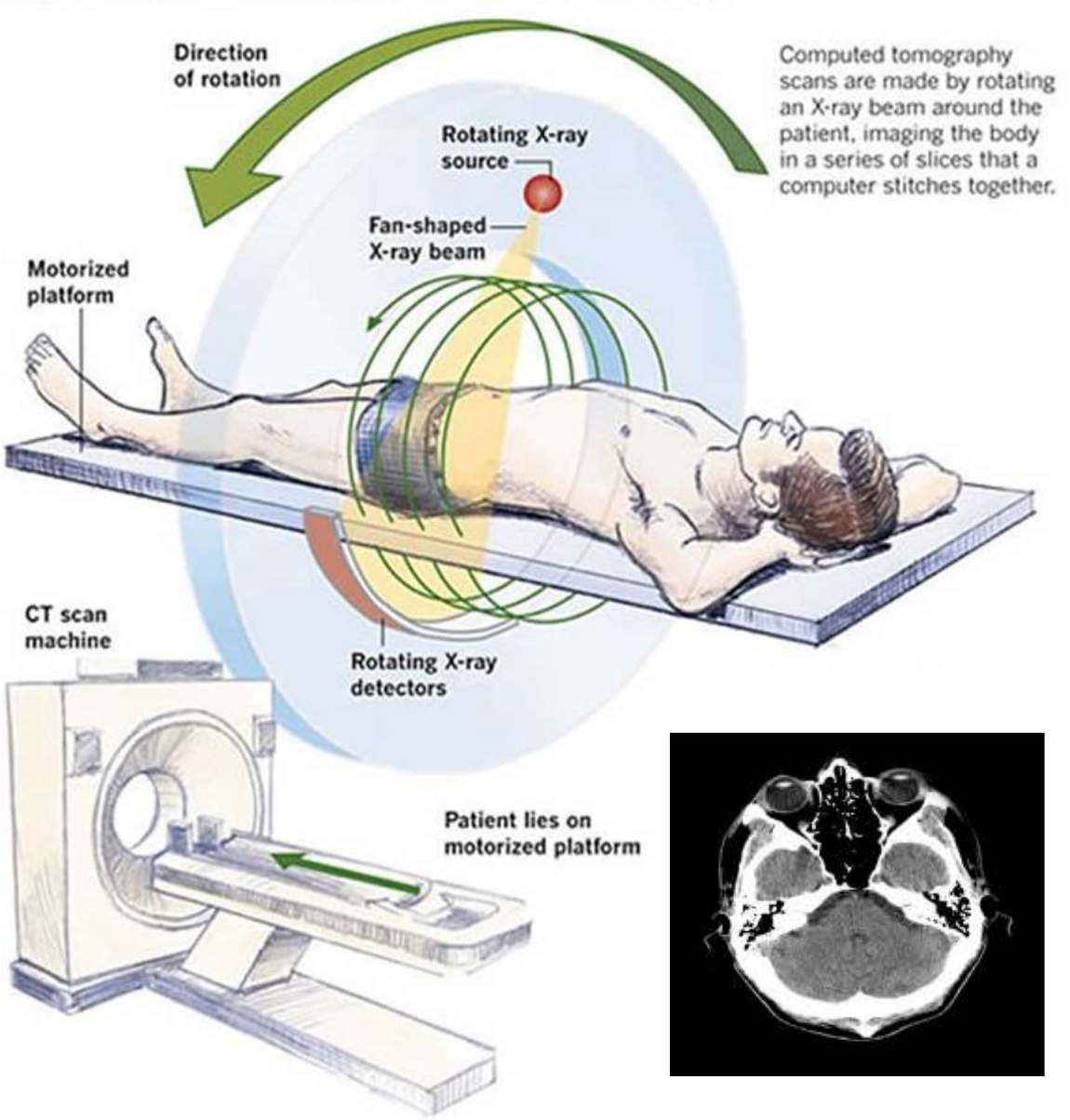

Figure 17. Diagram of computed tomography scanning system. (Inset, lower right) CT scan of the head showing the cerebellum, the orbits, the ethmoid sinuses, and a small portion of each temporal lobe.

In *computed tomographic angiography* (CTA), intravenous images are acquired in the arteries and reconstructed and displayed as 2D or 3D images. This technique is commonly used for imaging the aorta and renal and cerebral arteries. Contrast between different tissues of the body is improved by the use of various contrast media. These are high-molecular-weight substances that increase the opacity of the organ. CTA rapidly creates detailed pictures of the body, including the brain, chest, and abdomen. It is used in biopsies and to study blood vessels and identify masses and tumors.

8.3 Positron emission tomography (PET)

Positron emission tomography is a technique that allows measurements on distinct areas of the human brain while the patient is comfortable, conscious, and alert. While an X-ray or CT scan shows only structural details within the brain, PET gives a picture of the brain at work. To get these detailed pictures,

the radiation from the PET must interact with different substances. Oxygen-15 can be used for the study of oxygen metabolism, carbon monoxide for the study of blood volume, or water for the study of blood flow in the brain. Fluorine-18 can be attached to the glucose molecule to study the brain's sugar metabolism.

Working principle—A positron is an anti-electron or positively charged electron. Positrons are given off during decay of specific radioisotope nuclei. When matter collides with its corresponding antimatter, both are annihilated. When a positron meets an electron, the collision produces two gamma rays having equal energy, but emitted in opposite directions. The gamma rays are detected by the PET scanner. The scanner provides information to a computer that creates a complex picture of the patient's working brain (Figure 18).

The PET scanner uses radiation emitted from the patient to develop images. Each patient is given a minute amount of a radioactive pharmaceutical that closely resembles a natural substance used by the body. One example of such a pharmaceutical is 2-fluoro-2-deoxy-D- glucose (FDG), which is similar to a naturally occurring sugar, glucose, with the addition of a radioactive fluorine atom. Gamma radiation produced from the positron-emitting fluorine is detected by the PET scanner and processed to show the metabolism of glucose in the brain.

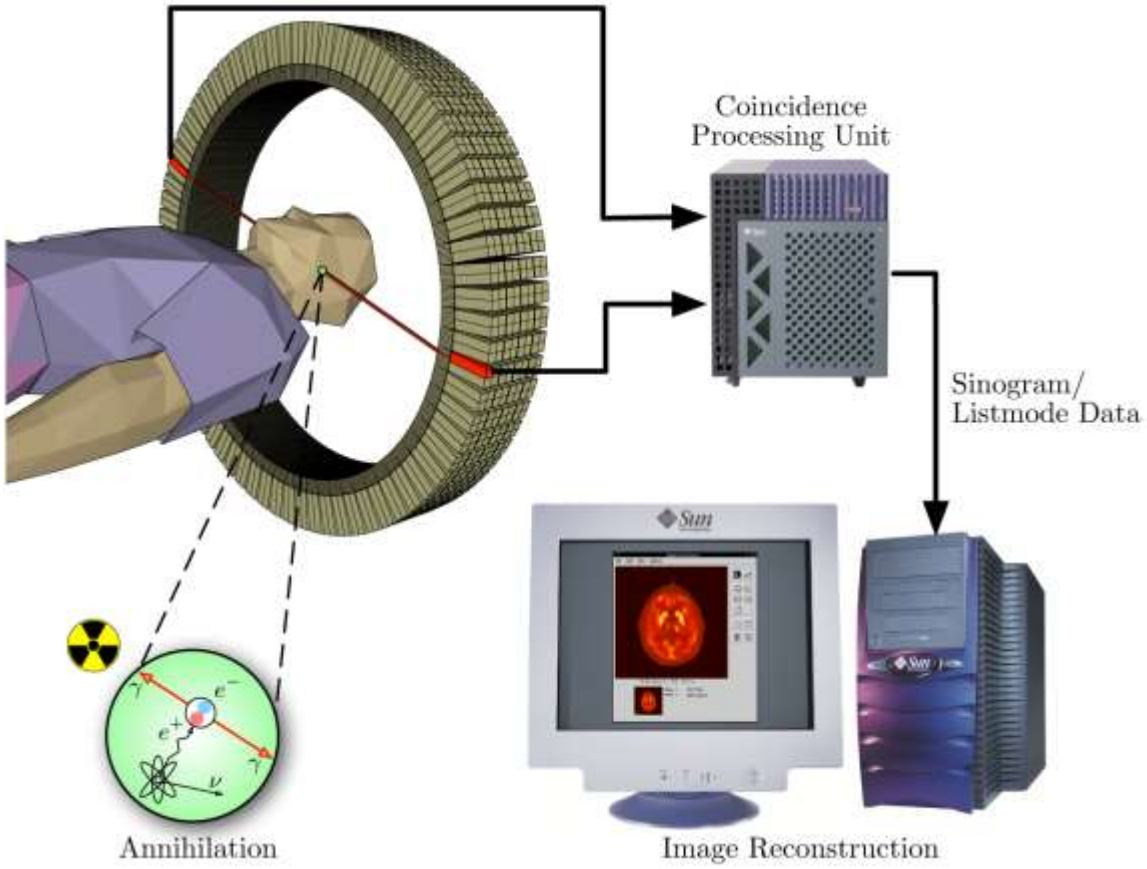

Figure 18. Diagram showing how a positron emission tomography system works.

Example 7
Use the formula, $E = mc^2$, to explain why during PET, a pair of positrons each with an energy of 511 KeV, are emitted. Assume that the mass of positron (a positively charged electron) is given by $m_p = m_e = 9.11 \times 10^{-31}$ kg. Also use the energy conversion of 1 eV = 1.6×10^{-19} J.

Solution
During PET, a positron, emitted during nuclear decay, travels a few millimeters, and then collides with an electron, resulting in emission of two high-energy 511 KeV photons. These photons travel in opposite directions, based on conservation of momentum. Their energy can be found by $E=mc^2$, where m is mass of two particles, a positron and an electron, that have been annihilated, and c is speed of light ($c = 3 \times 10^8$ m/s).
$E = mc^2 = (2)\ (9.11 \times 10^{-31}\ kg)\ (3 \times 10^8\ m/s)^2 = 1.64 \times 10^{-13}$ J.
$E = (1.64 \times 10^{-13}\ J)\ (1\ eV / 1.6 \times 10^{-19}\ J) = 1{,}025{,}000$ eV = 1025 KeV. Now, since there are two photons of equal energy given off, each photon has an energy of 1025 KeV / 2, or 512.5 KeV, which (considering rounding errors), is similar to the 511 KeV gamma ray photons emitted during PET procedures.

8.4 Single-photon emission computed tomography (SPECT)

Single-photon emission computed tomography (SPECT) is a nuclear medicine tomographic imaging technique that uses gamma rays to form images. It provides true 3D information on a specimen. This technique is employed in tumor imaging, infection imaging (leukocyte), thyroid imaging, and bone imaging. It is also used to provide information about localized functions in internal organs such as functional cardiac or brain imaging.

Working principle—SPECT imaging is performed by using a gamma camera to acquire multiple 2D images (also called projections) from multiple angles. The source of the gamma radiation detected by this camera is radionuclides that are contained in radiopharmaceuticals that are ingested by the patient. These pharmaceuticals are chosen on the basis of their ability to concentrate at locations within the body that must be examined. The gamma camera produces images of the distribution of these radionuclides. These images are processed by using a tomographic reconstruction algorithm that yields a 3D data set. This data set may then be manipulated to show thin slices along any chosen axis of the body, similar to those obtained from other tomographic techniques such as MRI, CT, and PET. Because SPECT acquisition is very similar to planar gamma camera imaging, the same radiopharmaceuticals may be used.

To acquire SPECT images, the gamma camera is rotated around the patient (Figure 19). Projections are acquired at defined points during the rotation, typically every 3–6 degrees. In most cases, a full 360-degree rotation is used to obtain an optimal reconstruction.

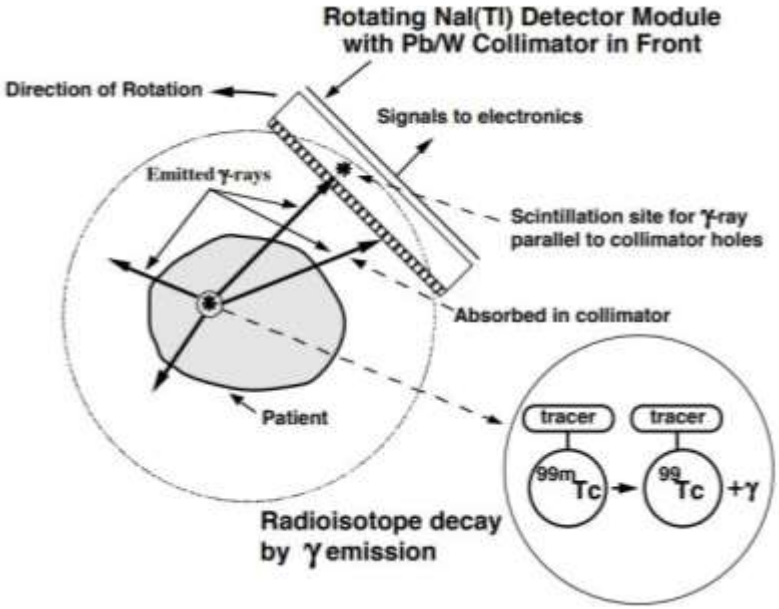

Figure 19. Diagram showing a single photon emission computed tomography system works.

Self-Test

36. What is a major advantage of using nuclear imaging (e.g. PET or SPECT)?
(a) Compact (b) Inexpensive (c) Good resolution (d) High contrast

37. Which of the following imaging modalities uses a positron as an intermediate step in imaging?
(a) PET (b) CT (c) SPECT (d) None of the above

38. What best describes a positron?
(a) Negatively charged proton (b) Neutron with electron's mass
(c) Positively charged electron (d) Hydrogen nucleus consisting of a single proton

39. Approximately how deep do positrons penetrate through the human body.
(a) 100 μm (b) 1 mm (c) 1 cm (d) Whole body

40. Approximately how deep do gamma ray photons penetrate through the human body?
(a) 100 μm (b) 1 mm (c) 1 cm (d) Whole body

41. What material provides the best protection from both x-rays and high energy x-rays (gamma rays)?
(a) Water (b) Soil (c) Lead (d) Wood

42. What is the approximate resolution of PET and SPECT nuclear imaging systems?
(a) 10 μm (b) 100 μm (c) 1 mm (d) 10 mm

9. Ultrasound (US)

9.1 Introduction

Although ultrasound (US) uses sound waves instead of electromagnetic waves for imaging, it is important to have a basic understanding of US imaging, for several reasons. First, US is often a first choice for diagnosis of many diseases and conditions because it provides good resolution (hundreds of micrometers), sufficient penetration depth for imaging entire organs (tens of centimeters), it is safe, compact, and inexpensive. Second, there are many similarities between the principles of US operation and how optical coherence tomography (OCT) works, the subject of the next section in this module. Third, one of the newest imaging modalities is photoacoustic imaging, which combines aspects of both optical imaging and US.

Ultrasound utilizes high frequency sounds waves, typically in the range of 1-20 MHz, for biomedical imaging applications. Sound waves are mechanical waves, which differ from electromagnetic (EM) waves in several important respects: (1) A mechanical disturbance is needed to create a sound wave, (2) Sound waves can only travel in a medium, not in a vacuum, (3) Sound travels much slower than light, approximately 1540 m/s in soft tissues, (4) Sound waves speed up in denser mediums while EM waves slow down, (5) acoustic impedance matching (e.g. use of a gel during fetal US) is necessary for sound waves to travel efficiently through interfaces between two different mediums (e.g. air and tissue).

The velocity, v_s, of sound waves is dependent on the density of tissue and is given by:

$$v_s = \lambda f \quad (15)$$

The acoustic impedance, Z, is given by the density (ρ) of a tissue times the speed of sound in the tissue:

$$(16) \qquad Z = \rho v_s$$

The source of contrast in an ultrasound image comes from the measured intensities of back-reflected sound waves, or echoes, due to the mismatch in acoustic impedances between two different tissues:

$$(17) \qquad I_r = [(Z_1 - Z_2) / (Z_1 + Z_2)]^2$$

Tissues with very different acoustic impedances (e.g. air and soft tissues, skull and brain tissues, lungs,..etc.) result in a high percentage of sound intensity being back-reflected and their interface, thus preventing deep imaging of subsurface organs. That is why a messy acoustic impedance matching gel needs to be placed on the skin during fetal US imaging, to eliminate air pockets between the US transducer and the skin. That is also why US is seldom used for diagnosis of brain tumors and lung cancer.

9.2 Resolution

The *axial resolution*, AR, in ultrasound is given by:

$$(18) \qquad AR = 3\lambda/2$$

where the number 3 comes from the fact that spatial pulse lengths (SPL) consisting of three wavelengths are typically used in each US pulse packet.

Similar to optical imaging, the *lateral resolution* in US is given by the spot diameter. Focused ultrasound beams are commonly used for imaging, and in such cases, in the near-field between the US transducer and the focal point, the beam is converging, resulting in a smaller spot and hence improved lateral resolution, while in the far field beyond the focal point, the beam is diverging, resulting in a larger spot and hence worse lateral resolution.

The axial and lateral resolutions, together, comprise two dimensions (Figure 20ab). The third dimension is given by the *elevational resolution*. The US transducer may consist of an array of many individual elements which can be activated independently or coordinated to electronically steer and focus the sound beam, as the individual US wavelets constructively or destructively interfere with each other (this is an example of Huygen's principle). The height of the individual US element provides the elevational resolution, which is usually constant based on the geometry of the US transducer (Figure 20c).

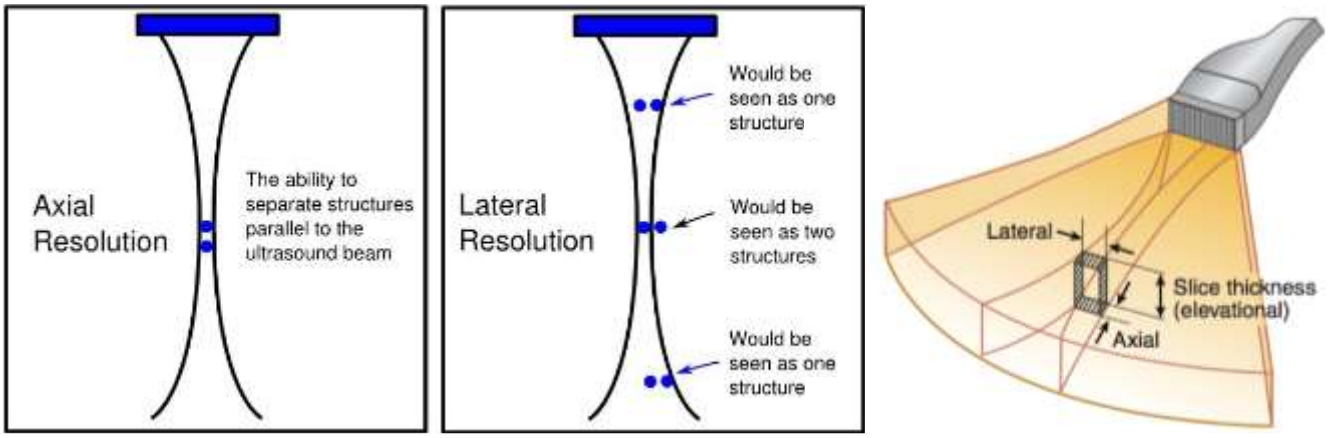

(a) (b) (c)

Figure 20. (a) Definition of axial and lateral (or transverse) resolution. (b) Orientation of axial, lateral, and elevational resolution for an US transducer. Axial resolution is determined by the frequency of US transducer, which in turn provides the wavelength for a given velocity in the tissue. Lateral resolution is given by the spot diameter and typically varies with depth in the tissue, as the US beam is focused and converging in the near-field, or diverging in the far-field. Elevational resolution is determined by the physical dimensions (height) of the individual elements which compose the array in the transducer.

Example 8
If an ultrasound transducer with a high frequency of 50 MHz is used for imaging, calculate the axial resolution for the ultrasound measurement. Assume that a speed of sound in soft tissue of 1540 m/s.

Solution
From equation 18, Axial resolution, AR = $3\lambda/2$. Also, from equation 15, $v_s = \lambda f$. First solve for λ, and then substitute the expression into the formula for axial resolution.
$\lambda = v_s / f$, so, AR = $3v_s / 2f$ = [3(1540 m/s)] / [2(50 x 10^6 Hz) = 4.6 x 10^{-5} m = 46 μm.

US imaging utilizes a transducer which acts as a sound source when it converts an electrical current into a mechanical wave through the rapid expansion and contraction of piezoelectric material. The same US transducer is usually used to image in reflection mode to wait for echoes (or reflected sound waves) to return from their roundtrip through the tissue. When these echoes of lower intensity sound waves impinge on the transducer, they then convert mechanical energy back into electrical energy and an electrical signal, which is used for reconstruction of the image. Hence, the US transducer acts as both an emitter and a detector.

The US technician chooses a specific type of transducer which emits at a central frequency, f. It is this variable that is controlled. For a given tissue, the speed of sound is constant, and therefore, the wavelength is indirectly determined from Equation 15, once the frequency of sound waves is chosen.

Ultrasound resolution and penetration depth both scale linearly with frequency, but in opposite directions (Figure 21). For example, US imaging that requires deep penetration of tissues (e.g. abdominal imaging and fetal US) uses an ultrasound transducer which emits a low frequency, which corresponds to a long wavelength. Such a wavelength results in less attenuation of the US intensity in the tissue, and results in deeper imaging depth, as required, but at the expense of worse axial resolution (since the wavelength is larger – see equation 18 above).

Conversely, US imaging that requires very good resolution typically sacrifices image depth. For example, US imaging of the eye (a relatively small organ) utilizes very high frequencies to make precise measurements of ocular structures. In general, the high frequency corresponds to a smaller wavelength (for better axial resolution), but also a smaller penetration depth due to increased scattering. However, for ophthalmic ultrasound applications, there is no scattering in the eye, which is transparent, so this is not a major limitation.

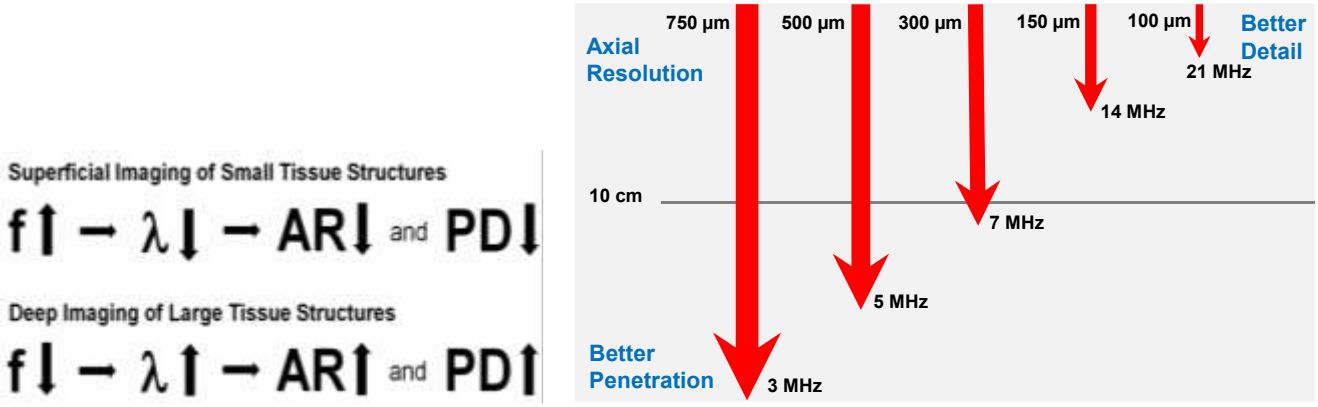

Figure 21. (a) The relationship between the chosen frequency of the US transducer, and the wavelength, axial resolution (AR) and image or penetration depth (PD). For deep imaging (e.g. fetal ultrasound), a lower frequency transducer is chosen to provide a longer wavelength, which translates into worse axial resolution (equation 18) and also less attenuation of the US beam due to scattering, resulting in deeper penetration depth. Conversely, a higher chosen frequency translates into a lower wavelength, resulting in better resolution but more scattering thus resulting in higher beam attenuation and lower penetration depth. (b) Diagram showing the trade-off between axial resolution and penetration depth as a function of US transducer frequency.

Ultrasound imaging is commonly performed in pulsed mode, in which short pulses on the order of a few microseconds are emitted, and then the majority of time is spent waiting for the reflected sound waves (due to differences in density at tissue interfaces), or echoes, to return.

The time delay, t, between sending and receiving US pulses is given by:

$$t = 2D / v_s \quad (19)$$

where D is the depth in the tissue. The value of 2D is used because the total path length of the sound wave is two times the depth in the tissue of the reflector, due to the roundtrip for imaging in reflection mode.

Example 9
If it takes 750 nanoseconds for an ultrasound wave to travel from the front surface to the back surface of the cornea, how thick is the cornea? Assume a sound velocity of 1540 m/s.

Solution
From equation 19, $v_s = 2D/ t$. Solve for D.
$D = v_s t / 2 = [(1540 \text{ m/s}) (750 \times 10^{-9} \text{ s})] / 2 = 5.78 \times 10^{-4} \text{ m} = 578 \text{ µm}$.

9.3 Image scanning modes

Ultrasound can be performed in different modes. The A-mode, or amplitude mode, involves a single line of data, from an US beam that is delivered into the tissue and then the echoes are collected (Figure 22). The peaks refer to a signal collected from a small amount of sound intensity that is back-reflected at the interface between two mediums with different densities (and hence different acoustic impedances as well). The valleys correspond to no signal, referring to areas within a given homogenous tissue or fluid

where there is no back-reflected beam or echo. The A-mode is not an image, but rather a one-dimensional mapping of the echoes as a function of depth (or depth profilometry). This information can be used to measure locations or distances, for example, the thickness of a tissue based on back-reflected peaks that occur at the front and back surfaces of the tissue.

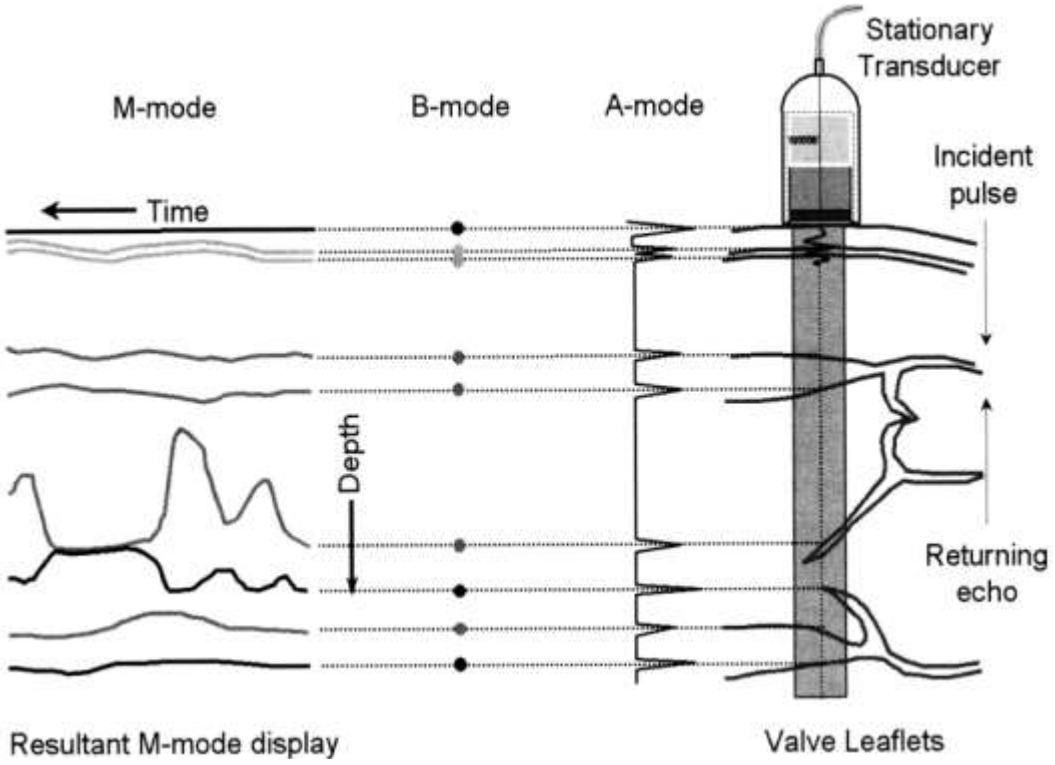

Figure 22. A-mode or “Amplitude” mode (series of reflected intensity peaks and valleys, not an image; used when accurate distance measurements are required, e.g. measuring cornea thickness). B-mode or "Brightness" mode (two dimensional image assembled from multiple A scans of data). T-M or M-mode, ”Time-Motion” mode (displays time evolution vs. depth, valuable for studying rapid movement, e.g. heart valve leaflets).

B-mode, or brightness mode, typically involves the collection multiple A-lines of data, and the representation of this data as spots of variable brightness (Figure 22). This data can be compiled into a gray scale or false color, two-dimensional image of a slice through the tissue (depth by lateral dimensions). Such images are what are shown on the monitor of an US machine.

M-mode, or motion mode, provides a time history of the location of back-reflections or echoes from the tissue, which may be useful in mapping anatomical objects with the body that rapidly move over time (e.g. heart valve leaflets opening and closing) (Figure 22).

The US image acquisition rate, or frame rate (in Hz or 1/s) is given by:

$$(20) \qquad FR_{max} = v_s / 2DN$$

where N is the number of A-lines of data.

9.4 Doppler Ultrasound

Ultrasound can also be used for *functional imaging*, or providing information on physiological changes in the body, besides standard anatomical imaging. A common example is Doppler US. When an object emitting sound waves is moving with respect to a listener, or vice versa, the same amount of wavelengths get either squeezed into a smaller space, for objects moving towards each other, or stretched into a larger space for objects moving away from each other. We experience this as a higher pitch or frequency when a car honks its horn as it drives towards us, and a lower pitch or frequency from the horn when the car drives away from us. Similarly, at very high US frequencies, a shift in the frequency can be detected from a moving object within the body. Doppler US can be used to measure the Doppler shift in frequency due to sound waves reflecting off of blood cells moving within our cardiovascular system.

The formula for the Doppler shift is given by:

$$(21) \qquad f_d = f_i - f_r = 2 f_i V_b \cos\theta / v_s$$

where V_b is the velocity of blood flow and θ is the angle between the US beam direction and the direction of blood flow (Figure 23).

This Doppler shift, which is measured, can then be used to calculate the velocity (both speed and direction) of the blood flow. This formula can be rearranged to solve for the blood flow:

$$(22) \qquad V_b = f_d v_s / 2 f_i \cos\theta$$

Doppler US information provides critical information on blood flow for diagnosing abnormal conditions in the cardiovascular tract.

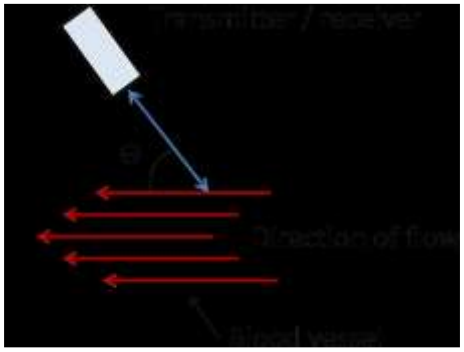

Figure 23. The angle, θ, is defined as the angle between the US transducer and the direction of blood flow.

Example 10
Compute the Doppler frequency shift due to a blood velocity of 30 cm/s for an ultrasound beam with an emission frequency of 3 MHz, incident on a blood vessel at an angle of 30 degrees with respect to the direction of the blood flow. Assume a speed of sound of 1540 m/s.

Solution
From equation 21, $f_d = 2 f_i V_b \cos\theta / v_s = [(2) (3 \times 10^6 \text{ Hz}) (0.3 \text{ m/s}) (\cos 30^o)] / (1540 \text{ m/s}) = 1.01 \times 10^3 \text{ Hz}$
So the Doppler frequency shift is approximately 1 KHz. This is an audible frequency.

9.5 Applications

Ultrasound is a widely used imaging modality due to its scalable and good resolution, moderate penetrate depth, safety, compact size, and low cost. Some of the most common applications include:

- Obstetrical US imaging for diagnosis and confirmation of early pregnancy, detection of fetal life signs, gestational size of fetus, location of placenta, multiple pregnancies, ectopic pregnancy,..etc.
- Gynecological US imaging for vaginal bleeding, cysts, and uterine fibroids.
- Echocardiography (US of the heart) for detecting blood clots that cause stroke, endocarditis, aortic aneurysm, coronary and congenital heart disease, heart attack…etc.
- Orthopedic US imaging for torn ligaments, nerves, muscles, and tendons in the ankle, elbow, knee, and shoulder. Image-guided needle drainage of fluids.
- Veterinary US using inexpensive handheld PC tablets in the field for portable diagnosis of abnormalities in large barnyard animals.

Self-Test

43. Which is a difference between light and sound waves?
(a) Light travels faster than sound (b) Sound waves need a medium to travel while light does not
(c) Light is a transverse wave while sound is a longitudinal wave (d) All of the above

44. During US imaging which type of resolution typically changes with depth into the tissue?
(a) Lateral resolution (b) Axial resolution (c) Elevational resolution (d) All of the above

45. As an US wave travels from one tissue to another inside the body, which physical parameter does not change?
(a) Wavelength (b) Frequency (c) Velocity (d) Acoustic impedance

46. As ultrasound frequency is increased, what happens to scattering of the sound waves in tissue?
(a) Increases (b) Decreases (c) Stays the same (d) Not enough information

47. The zone in which the US beam starts to diverge is called the _____.
(a) Near field (b) Far field (c) Axial zone (d) Lateral zone

48. Which of the following tissue components has the highest ultrasound attenuation?
(a) Water (b) Blood (c) Skin (d) Bone

49. During fetal US imaging, a gel is applied to the skin surface. What purpose does the gel serve?
(a) It provides matching of acoustic impedances between skin and US transducer
(b) It effectively increases the amount of US power transmitted into the subsurface tissue layers
(c) It allows for deeper imaging
(d) All of the above

50. The Doppler frequency shift is usually in what frequency range?
(a) Ultrasonic (b) Audible (c) Infrasonic (d) None of the above

51. To achieve a higher image frame rate, one can ____.
(a) Use fewer A-lines of data and image deeper into the tissue
(b) Use more A-lines of data and image deeper into the tissue
(c) Use fewer A-lines of data and image shallower into the tissue
(d) Use more A-lines of data and image shallower into the tissue

10. Optical Coherence Tomography (OCT)

10.1 Introduction

Optical coherence tomography (OCT) is a high-resolution, non-invasive optical imaging technique that utilizes back-reflected light at the interfaces between two tissues to reconstruct images, in an analogous way to ultrasound imaging. However, because the speed of light is approximately 3 x 10^8 m/s, orders of magnitude faster than the speed of sound in tissue (1540 m/s), it is not possible to use time-gating methods for optical imaging with high resolution the way that ultrasound uses time-gated sound waves (Figure 24).

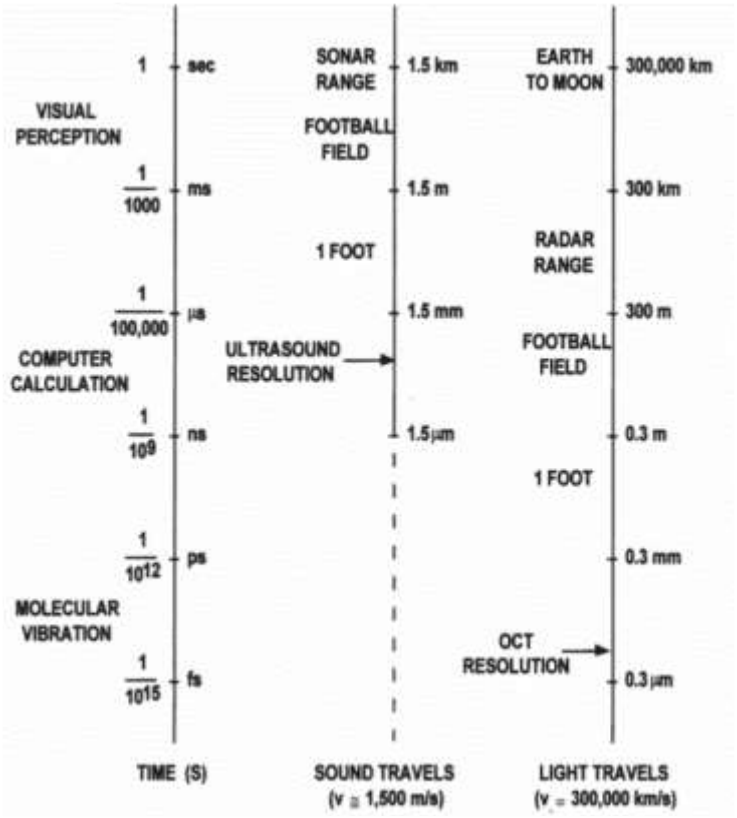

Figure 24. Comparison of resolution between ultrasound and optical coherence tomography. Since light travels so much faster than sound in tissue, it is not possible during OCT to use a time-gating technique like US does. Instead, the coherence properties of light and interferometric techniques are used to provide the very good axial resolution during OCT.

Instead, OCT uses an interferometric, noninvasive technique for imaging subsurface tissue structures with ultrahigh spatial resolution. OCT is based on the measurement of reflected or back-scattered light from differences in the refractive index, n, between two mediums at their interface. Since light scattering is orders of magnitude higher than scattering of sound waves, OCT is limited to superficial imaging depths of about 1-2 mm in turbid (opaque or non-transparent) tissues. Greater imaging depths can be achieved in transparent, non-scattering tissues such as the eye. OCT is therefore a widely accepted imaging technique in ophthalmology and has replaced US for imaging of many eye diseases. OCT provides at least an order of magnitude better resolution than US, and OCT can be used in non-contact mode, which is more comfortable for the patient's eye.

Table 9 provides a comparison of the technical specifications for OCT and US.

Table 9. Comparison of Optical Coherence Tomography and Ultrasound.

Properties	Optical Coherence Tomography (OCT)	Ultrasound (US)
Penetration depth	1-2 mm	Scalable (up to 10's of cm's)
Resolution	1-10 μm	100-500 μm
Mode	Non-contact	Contact
Wave speed	3 x 10^8 m/s	1540 m/s
Contrast	Light scattering	Acoustic scattering

10.2 Principle of operation

OCT actually uses an incoherent light source for imaging, rather than a coherent light source, such as a laser. The coherence length of the light (L_c) is inversely related to the linewidth of the light source (Figure 25).

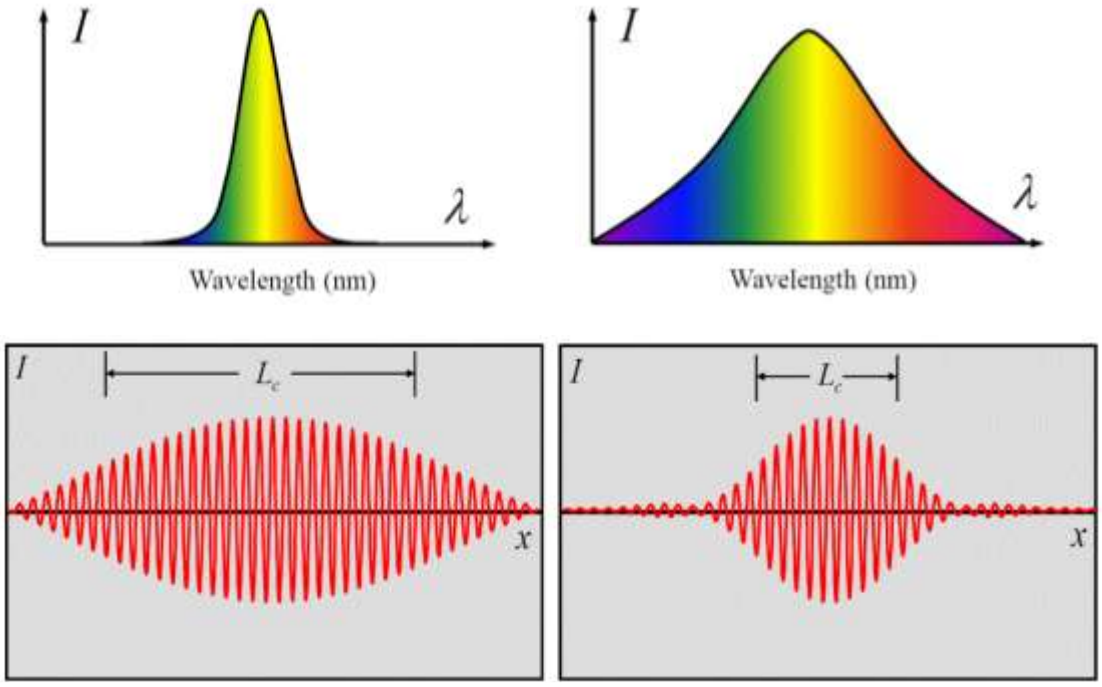

Figure 25. The coherence length of the light (L_c) is inversely related to the linewidth of the light source. For example, a narrow wavelength light source such as a laser is coherent, thus providing an infinite coherence length, and a very poor axial resolution, and thus is a poor source for OCT. Conversely, a light bulb is an incoherent light source which provides a very small coherence length, and thus a very good axial resolution. (However, light bulbs are not used for OCT due to the unfocused light properties.)

A narrow wavelength light source such as a laser is coherent and provides a very long coherence length, which translates into a very poor axial resolution for OCT. Instead, an incoherent light source which provides a very small coherence length is used during OCT to provide very good axial resolution. In theory, a light bulb which is a highly incoherent light source, could be used for OCT. However, since the light is emitted in all directions, the effective intensity at the tissue surface would be very low, and transmitting the light through an optical fiber for imaging inside the body would be very inefficient. In

practice, a compact, inexpensive, fiber coupled light source such as a superluminescent light emitting diode (SLED) is used for OCT.

The simplest configuration for OCT is that of standard Michelson interferometer (Figure 26). A beamsplitter is used to split the beam from the incoherent light source into two different paths: a sample path and a reference path. The sample path is the light that enters the tissue and is then back-scattered into the fiber again, and recombines with the light from the reference arm, which is back-reflected from a reflective mirror. When the two light beams recombine, there is a phase difference, which carries information about the tissue depth. Similar to how ultrasound works, the intensity of the back-reflected light from the tissue depends on the mismatch in the refractive index, n, at the interfaces between different tissue layers, and is thus the source of image contrast.

The intensity of back reflected light at the interface between two different tissues is given by:

$$I_r = [(n_1 - n_2) / (n_1 + n_2)]^2 \quad (23)$$

This formula is analogous to equation 17 for ultrasound, but with the acoustic impedance parameter, Z, replaced by the refractive index, n, instead.

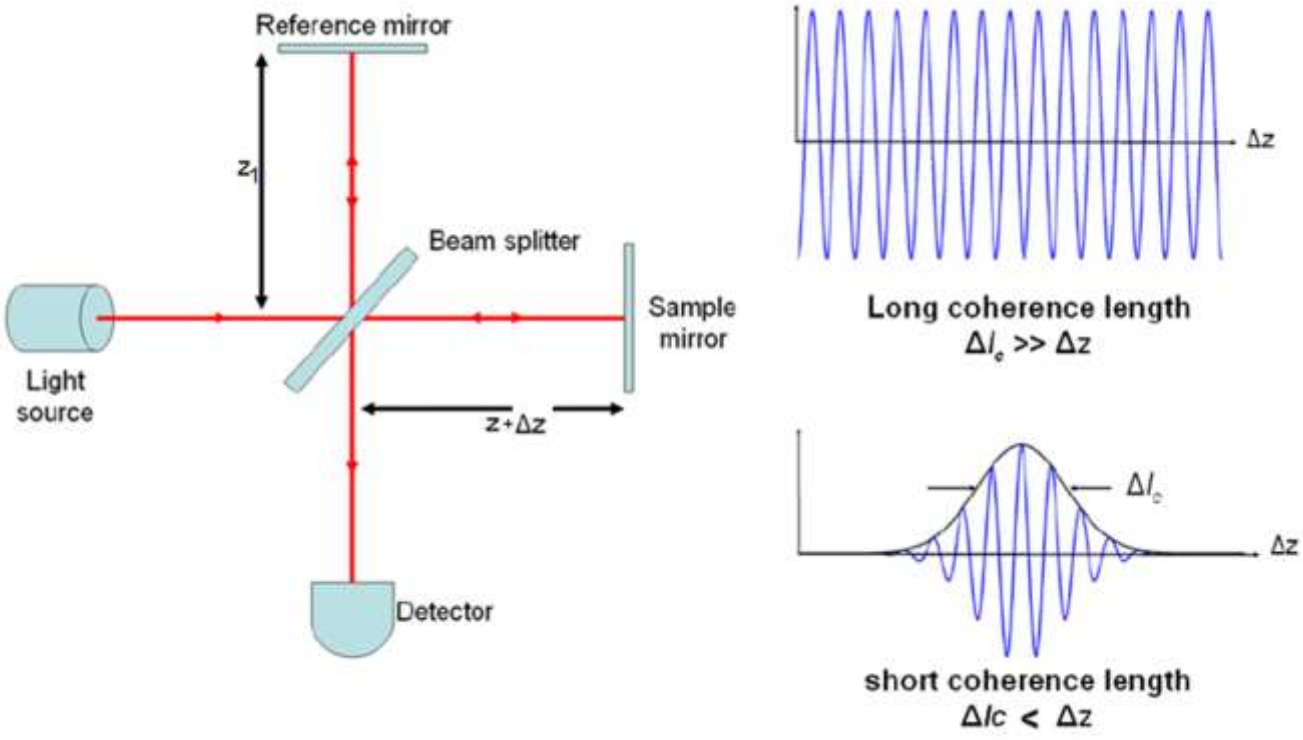

Figure 26. In its most simple configuration, an OCT system consists of a Michelson interferometer setup, where the incoherent light source beam is split into a sample path and a reference path using a beam splitter. The sample path is the light that enters the tissue and is then back-scattered into the fiber again, and recombines with the light from the reference arm, which is back-reflected from a mirror. When the two light beams recombine, there is a phase difference, which carries information about the tissue depth. The intensity of the back-reflected light from the tissue depends on the mismatch in the refractive index, n, at the interfaces between different tissue layers, and is thus the source of contrast in the image.

10.3 Resolution

Equation 24 and Figure 27 show how the optical bandwidth ($\Delta\lambda$) and wavelength (λ) of an OCT light source are related to the *Axial Resolution* (Δz):

$$(24) \qquad \Delta z = (L_c/2) = 2\ln 2/\pi\,(\lambda^2 / \Delta\lambda) = 0.44\,\lambda^2 / \Delta\lambda$$

When this equation is used with typical OCT values for $\Delta\lambda$ and λ, the depth at which details on an object can be resolved falls in the range of 1-10 μm. This calculation gives insight as to where OCT can be best applied.

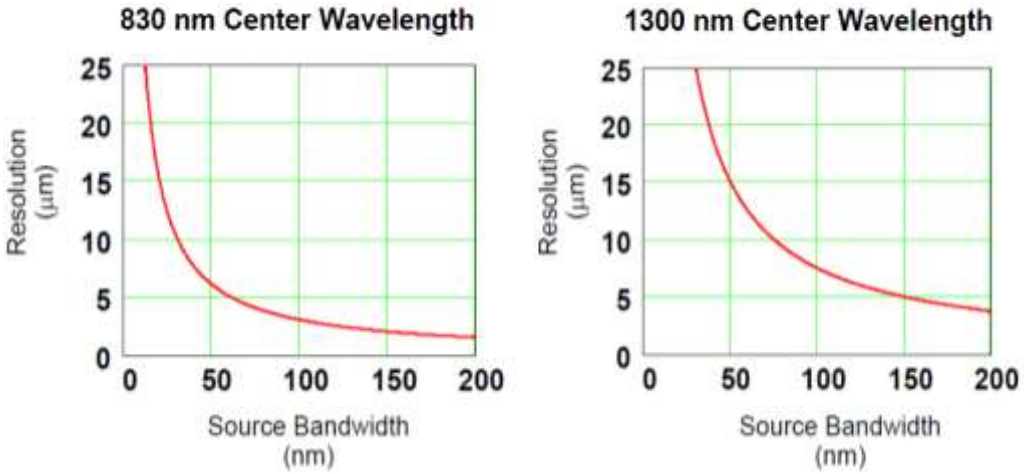

Figure 27. The axial resolution, Δz, is dependent on both wavelength, λ, and bandwidth, $\Delta\lambda$, of the light source. OCT light sources typically operates with center wavelengths in the near-infrared, from about 800-1300 nm, the "optical window" where light penetrates the deepest due to both limited absorption and scattering. Based on equation 24, a shorter wavelength and a larger bandwidth would provide the best axial resolution. Shorter center wavelengths (e.g. 830 nm) are typically used in ophthalmology where light scattering is absent, while longer center wavelengths (e.g. 1300 nm) are typically used for other applications involving opaque and highly scattering tissues (since light scattering decreases at longer wavelengths).

Example 11
If an OCT light source with a center wavelength of 850 nm and a bandwidth of 100 nm is used for imaging, calculate the axial resolution, and compare your value with that of ultrasound in example 8.

Solution
From equation 24, Axial resolution, $\Delta z = 0.44\,\lambda^2 / \Delta\lambda$
$\Delta z = 0.44\,(850 \times 10^{-9}\ \text{m})^2 / (100 \times 10^{-9}\ \text{m}) = 3.2 \times 10^{-6}\ \text{m} = 3.2\ \mu\text{m}$
The axial resolution of OCT is 3.2 μm while the axial resolution of high frequency ultrasound is 46 μm. OCT provides an axial resolution over an order of magnitude better than ultrasound. This characteristic has resulted in OCT replacing US for many imaging applications, especially in ophthalmology, since the eye is transparent, and the absence of light scattering enables deep OCT imaging with high resolution.

Transverse Resolution (Δx) is defined as focal diameter of incident beam and is not dependent on the coherence length of the source. The transverse resolution is given by:

$$(25) \qquad \Delta x = (4\lambda/\pi)\,(f/d)$$

Now, if from geometrical optics, the numerical aperture (NA), can be approximated as NA = nd / 2f, then simplifying produces f/d = n/2NA. Now, assuming that n = 1 for air, the term f/d = 1 / 2NA can then be substituted into the formula above to obtain the transverse resolution in terms of the numerical aperture:

$$(26) \qquad \Delta x = 2\lambda / \pi NA$$

Raleigh length (z_R) is defined as the distance along the propagation of the laser beam, measured from the beam waist (w_0) to the place where the area of cross section is doubled. For a Gaussian beam, the Raleigh length is given by:

$$(27) \qquad z_r = \pi w_o^2 / \lambda$$

The *Depth of Focus* in which lateral resolution is maintained is defined by the confocal parameter, b, (twice the Raleigh length), and is given by Equation 28 and Figure 28:

$$(28) \qquad b = 2\pi w_o^2 / \lambda \;=\; 2\pi\,(\Delta x/2)^2 / \lambda \;=\; \pi(\Delta x)^2 / 2\lambda$$

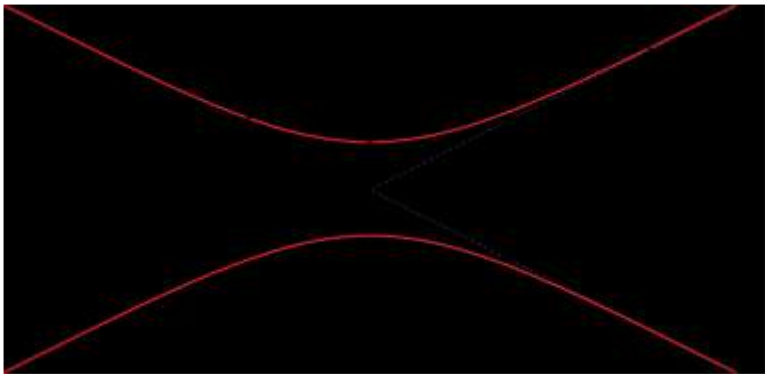

Figure 28. The depth of focus, also known as the confocal parameter, is related to the wavelength, and beam waist, which is turn also determines the traverse resolution.

Figure 29 summarizes the definitions and formulas associated with axial resolution, transverse resolution, and depth of focus for OCT.

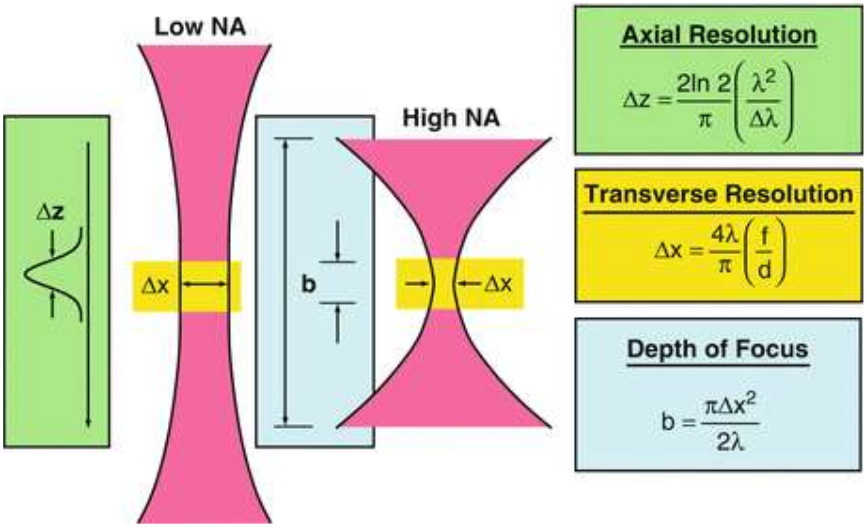

Figure 29. The main formulas relating axial resolution, transverse resolution, and depth of focus, as a function of wavelength, λ, bandwidth ($\Delta\lambda$), and numerical aperture, NA.

10.4 Image scanning modes

Again, similar to ultrasound, OCT can be performed in different scanning modes (Figure 30). An A-scan is a single line of data in the depthwise or z-direction, consists of a series of intensity reflection peaks and valleys, and essentially represents depth profilometry. The B-scan compiles a series of A-scans with lateral translation of the beam, to create a two-dimensional image of the tissue (depth times lateral cross-section). The C-scan, also known as *en face* imaging, consists of producing a two-dimensional cross-sectional image of the tissue at a fixed depth in the two lateral dimensions, essentially like how a confocal microscope performs optical sectioning of tissue.

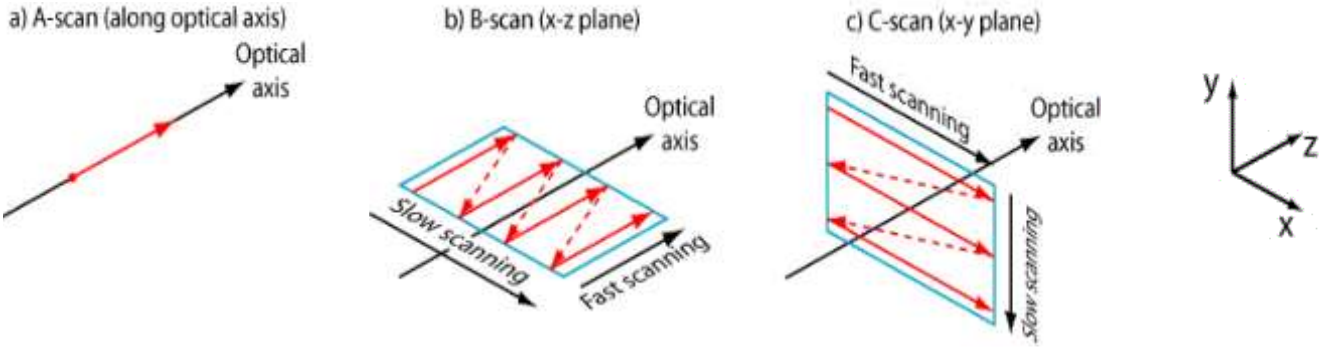

Figure 30. Classification of different OCT scans. An A-scan refers to a single line of data in the depthwise or z-direction, and consists of a series of intensity reflection peaks and valleys. The B-scan consists of a series of A-scans with lateral translation of the beam, to create a two-dimensional depthwise cross-sectional image of the tissue. The C-scan (*en face* imaging) consists of producing a two-dimensional cross-sectional image of the tissue at a fixed depth, much like how a confocal microscope works.

OCT is most commonly used in ophthalmology due to the absence of light scattering in a transparent tissue such as the eye. Figure 31 shows how A-scans in the eye can be used to measure the distances between different ocular structures, and B-scans can be used to reconstruct a two-dimensional image of the eye.

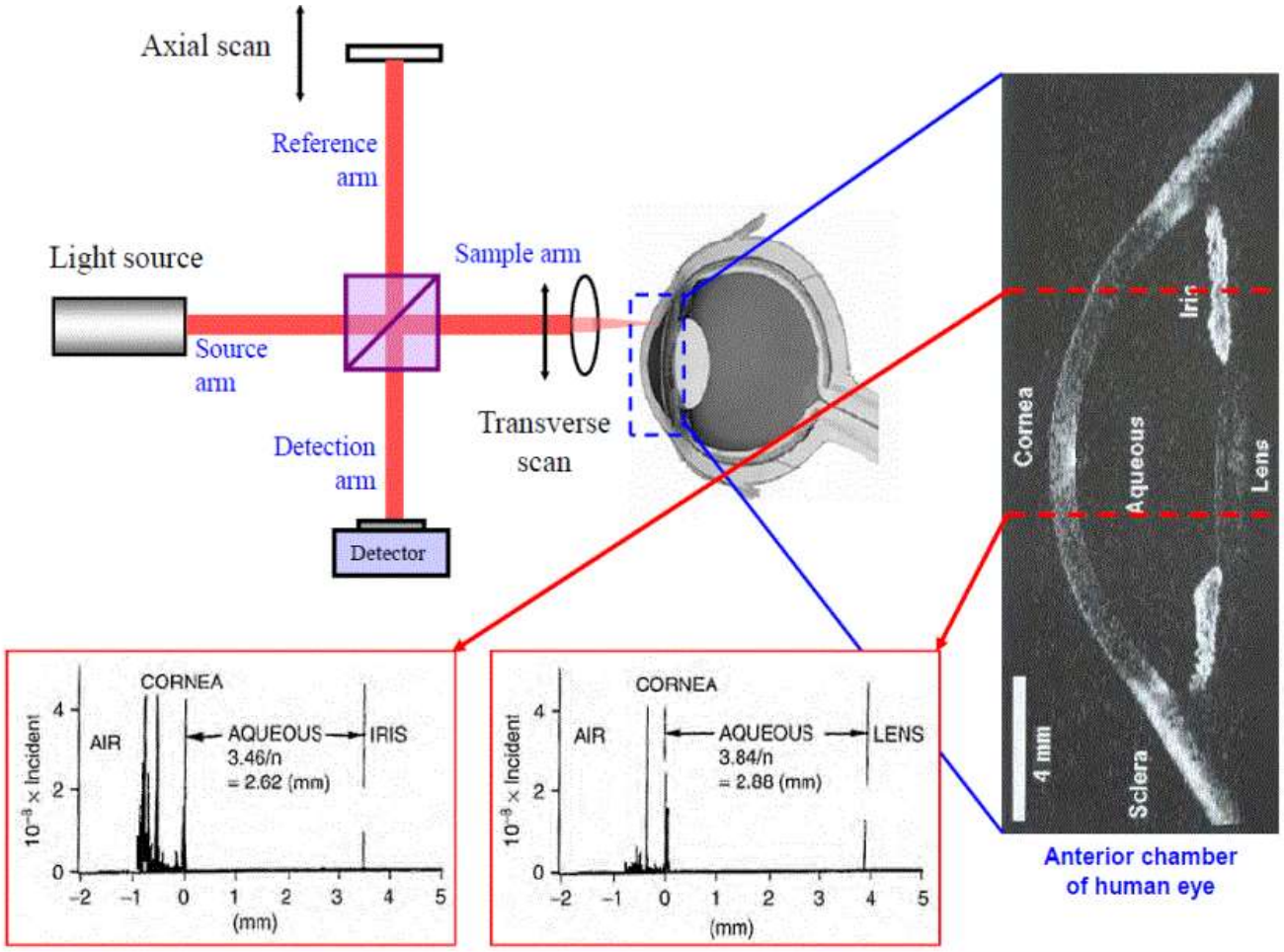

Figure 31. An example of OCT imaging in ophthalmology. Movement of the reference mirror in the interferometer configuration (top left) provides depth scanning through the tissue. The peaks represent back-reflections at the interfaces between air and tissue, or two different tissues. This A-scan data can be used to make precise measurements of tissue structure locations and thicknesses (bottom). The A-scans can also be used to reconstruct a two-dimensional image, or B-scan (right).

10.5 Doppler OCT

In an analogous manner to Doppler ultrasound, OCT can also be used to measure blow flow based on the Doppler effect, but on a smaller scale than Doppler US. For example, Doppler OCT can measure blood flow on the scale of 10 picoliters per second and in blood vessels as small as 10 micrometers in diameter. Potential clinical applications of Doppler OCT in measuring changes in the micro-vasculature in tissues, include optimization of port-wine stain therapy, photodynamic therapy, bleeding ulcers, burn depth analysis, and retinal blood flow analysis.

10.6 Applications

OCT has been employed in a variety of noninvasive diagnostic applications. Some of them are:

- In ophthalmology, OCT is used in diagnosing and monitoring retinal diseases such as glaucoma, macular edema, macular hole, central serous chorioretinopathy, epiretinal membranes, optic disc-pits, and choroidal tumors. Using OCT, parameters such as eye length can be accurately measured.

Cross-sectional images of the retina give a clear and quantifiable assessment of retinal separation and macular degeneration.

- In dermatology, OCT is used to diagnose skin diseases and detect skin cancer. OCT can be used to image the morphology of normal skin layers and components, and disorders such as psoriasis.
- In cardiovascular applications, OCT is used for detection of vulnerable plaque. This involves the study of how fluids, such as blood, travel through the body. Because these lesions are difficult to detect using conventional radiological techniques, OCT can be used to perform intracoronary imaging to identify high-risk *atherosclerotic plaques*. Although OCT's penetration is limited to a few millimeters, its resolution represents a 25-fold improvement over high-frequency ultrasound, MRI, and computer tomography.
- In combination with endoscopy, OCT is useful in the study of gastroenterology.

10.7 Laser Doppler velocimetry

The *Doppler effect* is the change in frequency and wavelength of a wave that is perceived by an observer moving relative to the source of the wave. This effect is demonstrated by the change in frequency of the sound a train makes as it approaches a person and then moves away.

Laser Doppler velocimetry (LDV) optically measures the velocity of a fluid without interfering with the fluid itself. The process measures the Doppler shift in wavelength of the laser radiation scattered by the moving particles. A monochromatic laser beam is directed at the target and the reflected light is collected. The change in wavelength of the reflected radiation is a function of the object's relative velocity. This velocity is given by:

$$v = f \lambda / 2\sin\theta \qquad (29)$$

where λ is the wavelength of the laser, *v* is the particle velocity, θ is the beam angle, and *f* is the frequency of the laser light that is reflected from the moving object. By measuring this frequency, the flow velocity can be measured. LDV typically uses a Helium Neon or Argon ion laser with a power of 10-20 mW.

Construction of a flow map using point measurement techniques such as LDV requires sequential measurements over a planar array of positions within the flow. This type of flow mapping can be performed using *planar Doppler velocimetry*. This technique determines the flow velocity by measuring the Doppler frequency shift of the light scattered by particles in the planar array. It utilizes a pulsed-injection-seeded Nd:YAG laser, one or two CCD cameras, and a molecular iodine filter. The laser illuminates a plane of the flow. The Doppler-shifted scattered light is then split into two paths using a beam splitter and imaged onto one or more cameras. Diagnostic applications

PDV is used in many diagnostic applications. Some of them are:

- Producing accurate assessment of blood flow and the velocity of blood in an echocardiogram
- Making velocity measurements of blood flow used in obstetric ultrasonography and neurology
- Determining circulation-associated fetal hypoxemia

Self-Test

52. The diagnostic window for deep optical imaging is what wavelength range?
(a) UV: 100-400 nm (b) Visible: 400-700 nm (c) Near-IR: 700-1300 nm (d) Mid-IR: > 3000 nm

53. Approximately how deep can OCT image in opaque tissues?
(a) 10-20 μm (b) 100-200 μm (c) 1-2 mm (d) 10-20 mm

54. Which is <u>not</u> an advantage of OCT over US imaging?

(a) Deeper penetration (b) Better resolution
(c) Use in non-contact mode (d) Use with small optical fiber delivery system

55. What is the typical axial resolution of an OCT system?
(a) 1-100 nm (b) 100-1000 nm (c) 1-10 μm (d) 100-1000 μm

56. A typical two-dimensional OCT image of depth versus lateral scan represents _____.
(a) A-scan (b) B-scan (c) C-scan (d) None of the above

57. To improve the axial resolution of an OCT system, one can ____.
(a) Use a shorter center wavelength and broader band light source
(b) Use a longer center wavelength and broader band light source
(c) Use a shorter center wavelength and narrower band light source
(d) Use a longer center wavelength and narrower band light source

11. Photon Migration Imaging

11.1 Ballistic photon imaging

When light is transmitted through a turbid medium, such as translucent biological tissues, some photons do not scatter but pass through. These are called *ballistic photons*. They follow the shortest path through the medium. Other photons in the light beam are scattered and move through the medium on paths that take them longer to transverse it. These photons are called *snake photons*. In biological tissue, scattering-absorption interactions complicate image reconstruction. The ability to separate out the ballistic and snake photons can lead to higher- quality images (Figure 32).

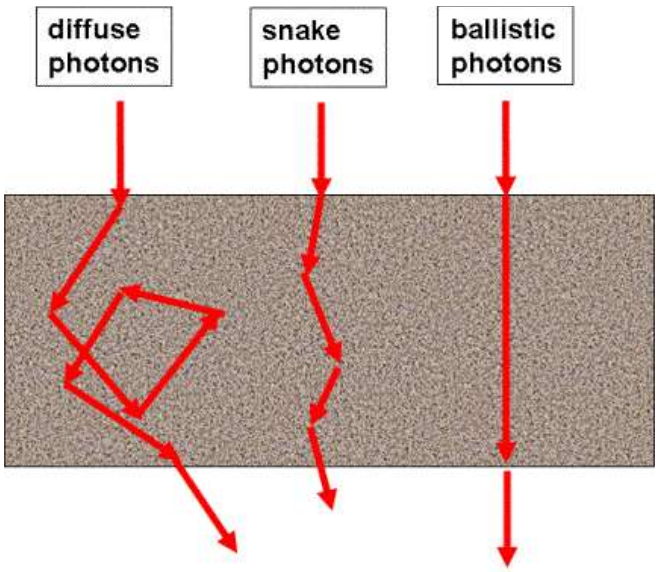

Figure 32. Classification of different photon paths through tissue. Diffuse photons undergo numerous scattering events as they travel through tissue, thus extending their total path length and time-of-flight through the tissue. Snake or quasi-diffusive photons wind their way through tissue with a shorter overall path length and time-of-flight. Ballistic photons, as the name suggests, travel like a bullet, on a straight

trajectory through the tissue, with minimal scattering, thus arriving first at the detector. Ballistic photon imaging exploits these differences in photon time-of-flight to reconstruct an image of the tissue.

Working principle—Ultrashort laser pulses that are used for optically scanning tissue have opened up the whole field of optical tomography. The basis for these techniques is the detection of *photons that travel ballistically* through tissue without scattering. Since they travel in a straight line, they arrive earlier at the detector than do the scattered photons. With sufficiently short pulses (around 30 ps), the ballistic photons can easily be separated from the slower, scattered ones (Figure 33). Ballistic photons can be used with optical tomography to scan the body in search of tumors or other abnormalities. They can also be used for spectral studies.

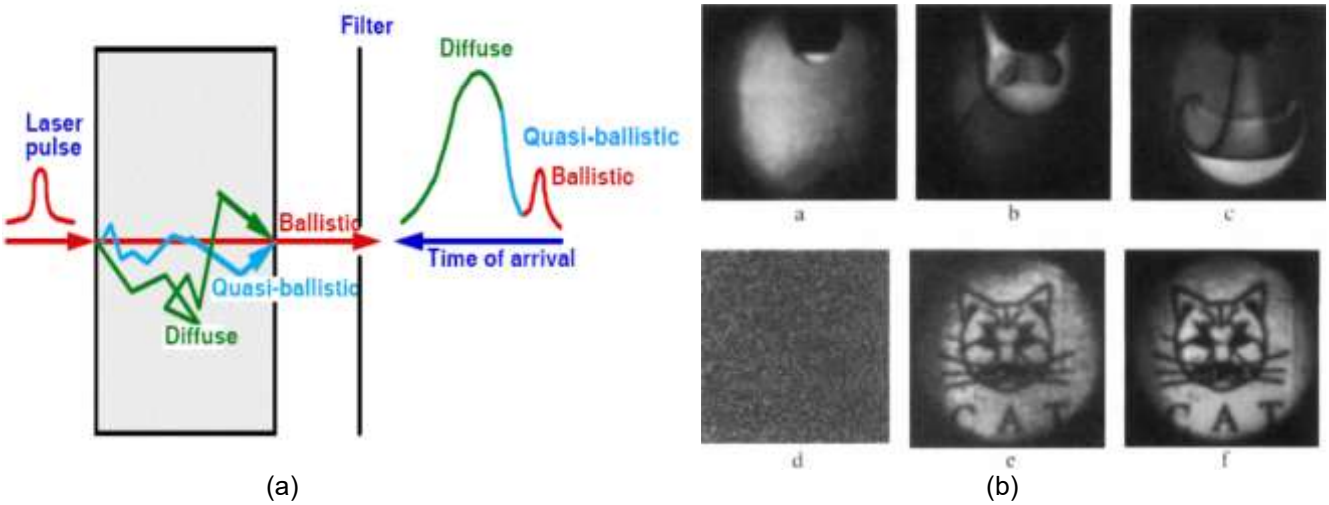

Figure 33. (a) Separation of ballistic, quasi-ballistic (snake), and diffuse photons, based on time of travel through a tissue. (b) "Alfano's cat", named after researcher Robert Alfano, is an example of ballistic imaging being able to reconstruct an image of a cat located in the subsurface layers of a tissue phantom.

In ballistic imaging, photon trajectories are easily traceable back to their points of origin. Image reconstruction is straightforward. Spatial resolution is very high, limited only by diffraction and coherence, and image quality is uniform throughout the sample.

However, this imaging technique is limited in that it requires a very expensive, short-pulsed laser source.

11.2 Diffuse optical tomography (DOT)

Diffuse optical tomography (DOT) refers to the use of near-infrared optical imaging in the diffusive regime where there is a high number of photon scattering events, or multiple light scattering. DOT applications include functional imaging of large, thick tissues, for example, tumors in the brain or breast. Unlike, OCT, which is a high resolution imaging technique because the image depth is several orders of magnitude greater than the spatial resolution, DOT is referred to as a low resolution imaging technique, because spatial resolution is only about 20% of the imaging depth. In a DOT system, sources and detectors are placed around object to be imaged in various geometric configurations (Figure 34). While one source illuminates object, all detectors measure re-emitted light. This process is repeated with each source to complete a measurement data set, then images reconstructed by computer.

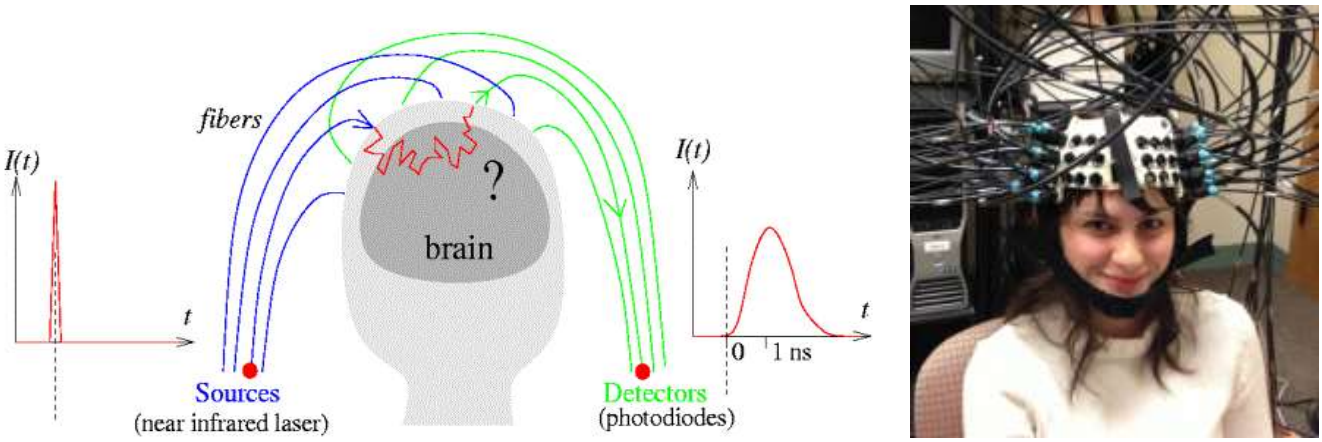

(a) (b)

Figure 34. During DOT, multiple light sources and detectors are placed around the tissue of interest, as shown in the (a) diagram and (b) photograph.

Three DOT Modes include continuous-wave, frequency-domain, and time-domain.

For continuous-wave DOT, data is acquired in the form of light intensities. Image quality depends on source-detector density. Simultaneous reconstruction of absorption and reduced scattering coefficients is difficult. Data acquisition is fast, the hardware is simple and low cost (e.g. diode lasers and photodiode detectors).

For frequency-domain DOT, intensity modulated light source provide data in the form of both amplitude and phase. Data acquisition is slower than continuous-wave DOT, but image quality is better, and hardware is more expensive.

For time-domain DOT, data acquisition is the slowest, but the image quality is the highest. However, the hardware is the most sophisticated and expensive (e.g. ultrafast pulse light source and time-correlated single photon counting).

Figure 35 shows the data acquisition for these three DOT techniques.

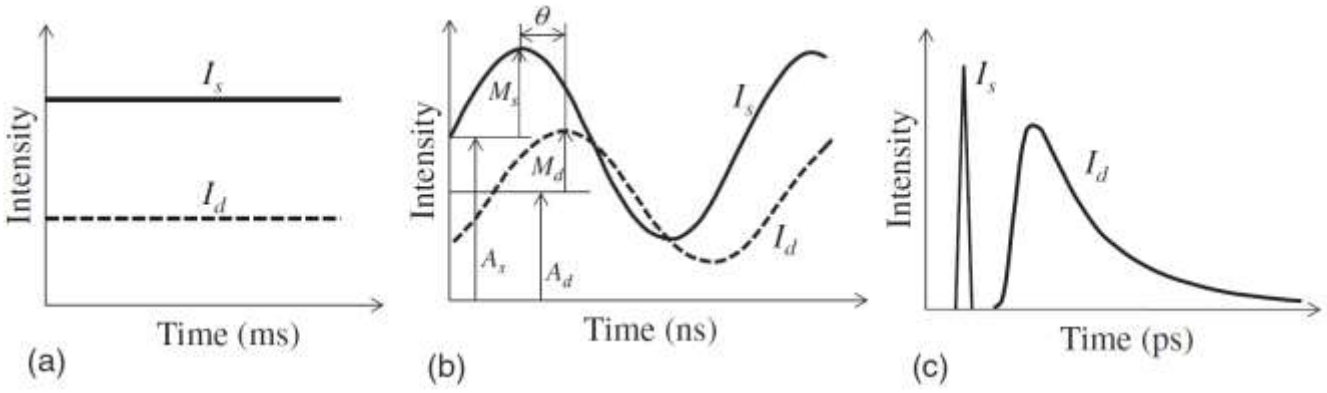

Figure 35. Comparison of data acquisition with three diffuse optical tomography techniques. (a) Continuous-wave; (b) Frequency-domain; and (c) Time-domain.

Self-Test

58. Which types of photons take the longest time to be transmitted through a tissue?

(a) Ballistic (b) Diffuse (c) Snake (d) Quasi-diffuse

59. Which DOT technique uses the most simple and low cost laser sources and detectors?
(a) Continuous-wave (b) Frequency-domain (c) Time-domain (d) It depends

60. Which DOT technique provides the highest image quality, but requires the most sophisticated and expensive laser sources and detectors
(a) Continuous-wave (b) Frequency-domain (c) Time-domain (d) It depends

12. Photoacoustic Imaging

12.1 Introduction

Photoacoustic imaging, as the name suggests, combines aspects of both optical imaging and ultrasound imaging. Photoacoustic imaging fills a missing gap not currently covered by other imaging modalities. For example, optical coherence tomography (OCT) is capable of imaging very small structures at cellular level resolution, but is limited by superficial penetration depths, due to multiple light scattering attenuating the signal. Conversely, diffuse optical imaging provides much deeper imaging depth but at the expense of poor resolution. Ultrasound (US) imaging suffers from poor contrast. Both OCT and US are limited by speckle artifacts. By exciting the tissue with light, photoacoustic imaging provides increased contrast over US, and by detecting acoustic waves, instead of light, deeper imaging can be performed with much less attenuation of the signal because ultrasound scattering is much less than light scattering in tissues. In effect, photoacoustic tomography provides better resolution than diffusing optical imaging techniques and better imaging depth than optical coherence tomography (see Figure 1 comparing resolution and penetration depth of all imaging modalities). The resolution of photoacoustic images is scalable based on the ultrasound frequency chosen for detection, similar to conventional ultrasound imaging (see Figure 21 in US section).

12.2 Principle of operation

Photoacoustic imaging works by using short-pulses emitted by a laser, typically a frequency-doubled Nd:YAG laser at a green wavelength of 532 nm. The low energy light is selectively absorbed by a chromophore or absorber in the tissue (e.g. hemoglobin selectively absorbs green light). As the light is absorbed, the targeted tissue expands through thermoelastic expansion. This expansion creates acoustic waves that can be picked up by very sensitive ultrasound detectors (Figure 36).

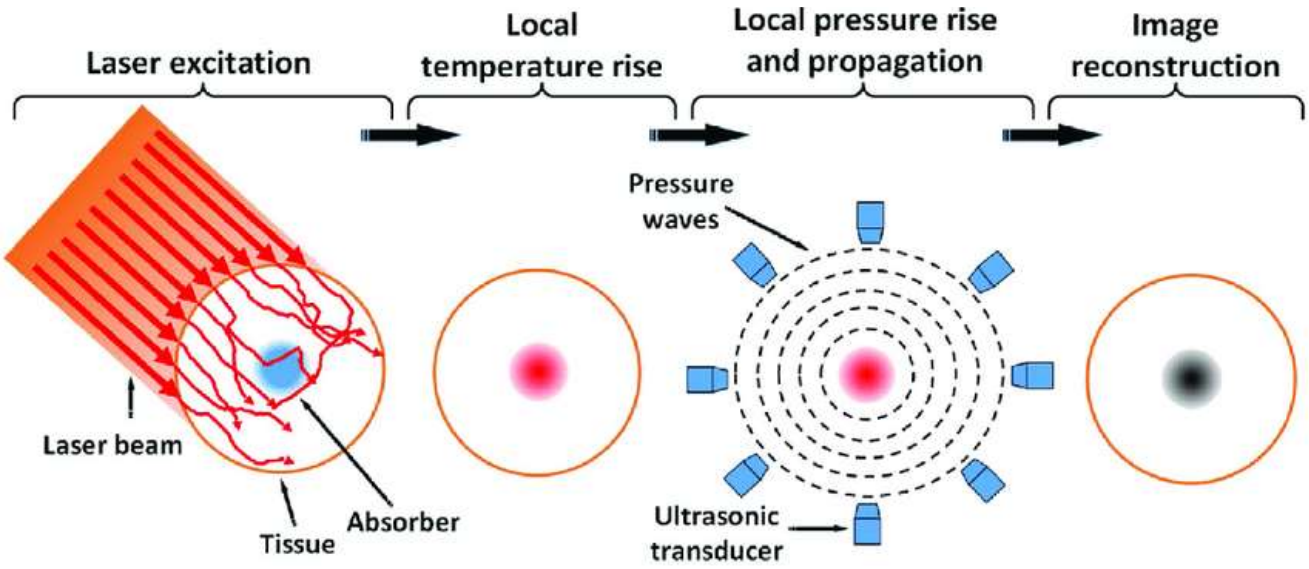

Figure 36. Diagram and steps provided for photoacoustic tomography.

Photoacoustic tomography has some limitations. For example, the Q-switched laser source used is significantly more expensive than superluminescent diode (SLD) sources used in OCT and US transducers. Some of the limitations of conventional ultrasound also still apply including the need to use an acoustic impedance matching agent to insure contact between the US transducer and the tissue, as well as the inability to image through certain tissue that have either large intensity losses due to acoustic impedance mismatches at tissue interfaces (e.g. skull and brain tissue) and high sound intensity attenuation within the tissues themselves due to absorption (e.g. bones) or scattering (e.g. lungs).

Table 10 summarizes some of the advantages and disadvantages of photoacoustic tomography.

Table 10. Summary of Advantages and Disadvantages of Photoacoustic Tomography

Advantages	Disadvantages
Improved resolution compared to DOT	Expensive, short-pulse laser source necessary
New contrast (e.g. hemoglobin) compared with US	Need 360° access to tissue for imaging
Deeper tissue imaging than OCT	Need selective optical absorber in the tissue
No speckle artifacts, unlike US and OCT	US waves used for detection do not easily penetrate some tissues such as skull and lungs
Functional imaging with endogenous contrast agents	US detector needs to be in contact with tissue
Molecular imaging with exogenous contrast agents	
Non-ionizing radiation, unlike x-rays/CT, SPECT/PET	

12.3 Photoacoustic microscopy

A photoacoustic microscope utilizes photoacoustic imaging and detected sound waves emitted at very high frequencies, to provide better resolution than conventional ultrasound while also providing better

imaging depth than conventional optical imaging techniques such as confocal and two-photon (or multiphoton) microscopy and optical coherence tomography (Table 11).

Table 11. Comparison of Photoacoustic Microscopy to Other Techniques

Imaging Modality	Primary Contrast	Image Depth (mm)	Resolution (μm)
Confocal microscopy	Fluorescence/Scattering	0.2	1-2
Two-photon microscopy	Fluorescence	0.5	1-2
Optical coherence tomography	Optical scattering	1-2	10
Ultrasound (5 MHz)	Acoustic scattering	60	300
Photoacoustic microscopy (50 MHz)	Optical absorption	3	15
Photoacoustic tomography (3.5 MHz)	Optical absorption	50	700

Figure 37 shows a representative photoacoustic microscopy experimental setup as well as images providing quantitative measurements of hemoglobin concentration, blood oxygenation levels, and blood flow rates.

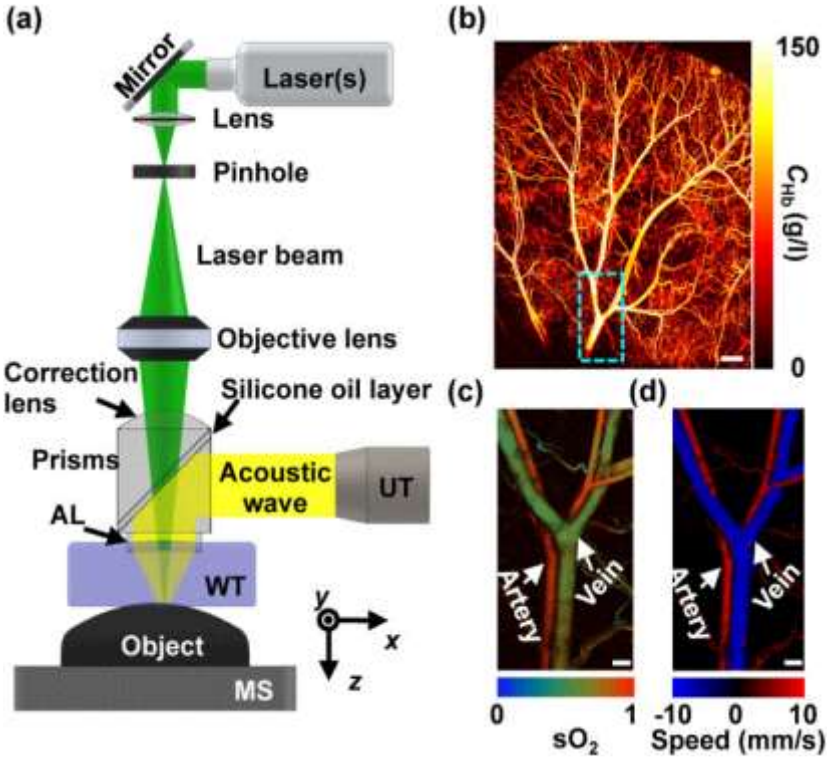

Figure 37. (a) Diagram of components in a photoacoustic microscopy system, used to measure (b) concentration of hemoglobin (CHb) in mouse ear, (c) oxygen saturation (sO_2), and (d) blood flow (mm/s).

Example 12
A Q-switched, frequency doubled Nd:YAG laser is tested for photoacoustic tomography of blood vessels in port-wine stains. The laser has a wavelength of 532 nm and pulse duration of 10 ns. Assume that radiant exposure or fluence (F) at the blood vessel is 10 mJ/cm^2, and that the average blood vessel diameter is 100 μm. Based on these specifications, answer following questions:

(a) Calculate the thermal relaxation time using equation, $\tau_{th} = d^2 / 4\kappa$, if thermal diffusivity is $\kappa = 1.5 \times 10^{-3}$ cm^2/s , and answer if thermal confinement is achieved during laser pulse.

(b) Calculate the stress confinement time using equation, $\tau_{st} = d / v_s$, where average speed of sound in soft tissues is $v_s \sim 1540$ m/s, and answer if acoustic confinement is achieved.

(c) Calculate the temperature rise using $\Delta T = \mu_a F / \rho c$, where the absorption coefficient of blood at λ = 532 nm is $\mu_a = 200\ cm^{-1}$. Assume a density, $\rho = 1\ g/cm^3$, and heat capacity, c = 4.2 J / g-°C. and answer whether this temperature rise is safe for imaging the tissue.

(d) Calculate the initial photoacoustic pressure generated using equation, $p_0 = \beta \Delta T / k$, where the isothermal compressibility is $k = 5 \times 10^{-10}$ $Pascals^{-1}$, and thermal coefficient of expansion is $\beta = 4 \times 10^{-4}\ K^{-1}$, and your answer for ΔT, from part (c) above. (0°C = 273 K).

(e) Assuming that an axial resolution of about 100 μm is desired, calculate approximate frequency of US transducer used for detection.

Solution
(a) d = 100 μm = 0.01 cm and $\kappa = 1.5 \times 10^{-3}\ cm^2/s$, so
$\tau_{th} = d^2 / 4\kappa = (0.01\ cm)^2 / 4(1.5 \times 10^{-3}\ cm^2/s) = 1.7 \times 10^{-2}$ s = 17 ms
Laser pulse duration is τ = 10 ns, so $\tau < \tau_{th}$ and Yes, thermal confinement is achieved.

(b) $\tau_{st} = d / v_s = (0.01\ cm) / 1.54 \times 10^5\ cm/s = 6.5 \times 10^{-8}$ s = 65 nanoseconds
$\tau < \tau_{st}$ so Yes, acoustic confinement is achieved.

(c) The fluence is $F = 10\ mJ/cm^2 = 0.01\ J/cm^2$
$\Delta T = \mu_a F / \rho c = (200\ cm^{-1})\ (0.01\ J/cm^2) / (1\ g/cm^3)\ (4.2\ J / g\text{-}°C) = 0.5$ °C
Yes, this is a negligible temperature increase and is safe.

(d) $p_0 = \beta \Delta T / k = (4 \times 10^{-4}\ K^{-1})\ (0.5\ K) / (5 \times 10^{-10}\ Pa^{-1}) = 4.0 \times 10^5$ Pa = 400,000 Pa = 4 bars

(e) Ultrasound Axial Resolution = $3\lambda / 2$ = 100 m.
So, $\lambda = (2/3)$ (100 μm) = 67 μm
$\lambda f = v_s$, so $f = v_s / \lambda = (1540\ m/s) / (6.7 \times 10^{-5}\ m) = 2.3 \times 10^7$ Hz = 23 MHz

12.4 Applications

Photoacoustic imaging is used to detect vascular disease, skin abnormalities, and some types of cancer. The high-resolution capability of the photoacoustic system makes it particularly well suited to clinical dermatological applications that require visualization of blood vessel networks and healing wounds. It is also useful in the study of molecular imaging in cardiovascular studies, neurology, and oncology. Hemoglobin (and its various oxygenated states) provides strong optical contrast at near-IR and visible wavelengths, making the technique well suited for imaging blood vessels (Figure 38).

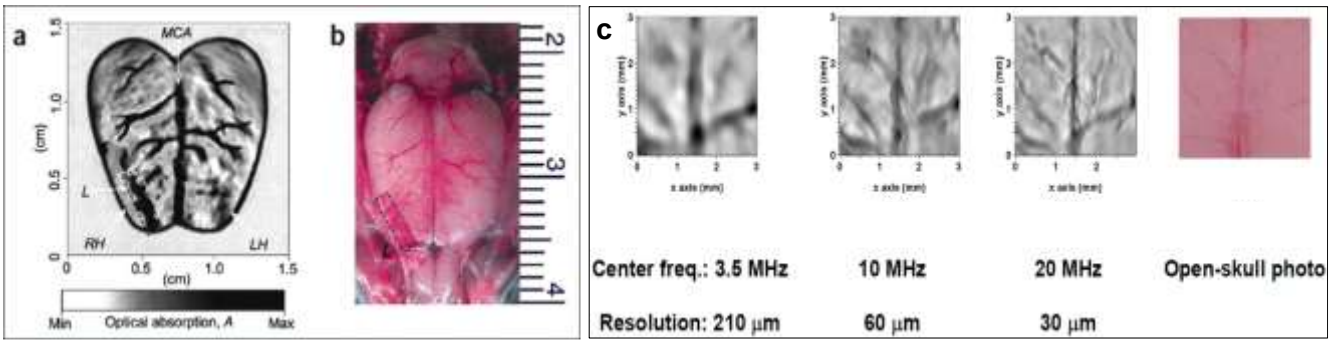

Figure 38. (a) Image of a lesion in the rat brain using a Q-switched Nd:YAG laser with a wavelength of 532 nm, pulse duration of 6.5 ns, and pulse rate of 10 Hz. (b) Photograph of the lesion for comparison. (c) Images of blood vessel in the brain, showing trade-off between US frequency and image resolution.

Self-Test

61. Which color of light is strongly absorbed by blood during photoacoustic imaging?
(a) UV (b) Green (c) Red (d) Infrared

62. Which is an advantage of photoacoustic imaging over ultrasound and optical imaging?
(a) Better resolution than diffuse optical imaging (b) Better penetration depth than OCT
(c) Better contrast than ultrasound (d) All of the above

63. During photoacoustic imaging, what is the detected?
(a) A weak light signal (b) A weak ultrasonic wave (c) A ballistic photon (d) None of the above

64. A major limitation of photoacoustic imaging is the need to ____.
(a) Use an expensive short-pulse laser source (b) Place the tissue in contact with the US transducer
(c) Have selective absorber of light in tissue (d) All of the above

Answers to Self-Tests

1. c	2. b	3. d	4. d	5. d	6. d	7. a
8. c	9. b	10. b	11. a	12. a	13. c	14. b
15. a	16. c	17. b	18. d	19. c	20. d	21. d
22. d	23. c	24. a	25. d	26. b	27. c	28. d
29. a	30. a	31. d	32. b	33. b	34. c	35. a
36. d	37. a	38. c	39. b	40. d	41. c	42. d
43. d	44. a	45. b	46. a	47. b	48. d	49. d
50. b	51. c	52. c	53. c	54. a	55. c	56. b
57. a	58. b	59. a	60. c	61. b	62. d	63. b
64. d						

The following two laboratories give students an opportunity to gain a hands-on experience in understanding the principles underlying filters and lenses. These two areas are keys to mastering the material presented in this module.

Laboratory 1: Absorption and Transmission of Optical Filters

Sunglasses and brake light filters are both examples of optical filters. They both absorb and transmit a portion of incident light. The difference is that sunglasses are independent of wavelength. They equally absorb and transmit all wavelengths. A brake light filter is wavelength dependent: It transmits only red light and absorbs all other colors. The absorption of light through a material is based on the exponential law of absorption given by the following equation:

$$E = E_o e^{-\alpha x}$$

where

E = transmitted irradiance,
E_o = incident irradiance,
α = absorption coefficient cm^{-1}, and
x = thickness in cm.

The transmission (T) can be calculated using the following equations:

$$T = E/E_o = e^{-\alpha x} \text{ (no units)}$$

The absorption coefficient can be found by:

$$\alpha = -(\ln E/E_o)/x$$

A plot of the transmitted light versus filter thickness is shown in Figure L1. The slope of the curve is the absorption coefficient. The absorption coefficient is a constant based on the material. The material can be wavelength dependent.

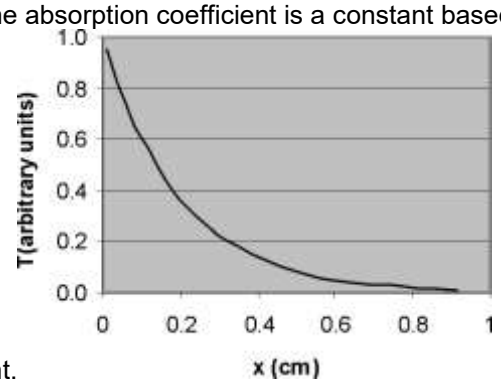

Figure L1 *Transmitted light versus filter thickness*

Objectives

- Measure the transmission of optical filters as a function of filter thickness.

- Calculate the absorption coefficient α of each filter type using the exponential law of absorption

Equipment

HeNe laser
Optical power meter
Broadband plastic filters
Lab jack
Filter mount
Neutral density filters
Diverging lens
Micrometer
Lens mount

Procedure

1. Plug in laser and carefully place on lab jack.
2. Holding only the edges of the diverging lens, insert into lens holder
    a. Place lens holder into the path of the laser approximately 5 cm from the aperture of the laser.
3. Observing safety precautions, turn on laser.
    a. Make sure the reflected beams from the lens are directed back into the aperture of the laser.
    b. The laser beam must be incident on the center of the lens for proper alignment.
4. Turn on power meter.
    a. Set λ = 633 nm. In the wavelength (λ) calibration mode, the number on the meter will indicate the λ in nm. After exiting this mode, the number will indicate power ranging from μW to mW depending on range chosen.
    b. Press λ button to exit wavelength calibration mode and initially set range to 3 mW
    c. Press zero on meter (negates background light).
5. Measure the power (P_o) and calculate the irradiance (E_o) at a distance where the beam fills the area of the detector. Record in Data Table L1. The irradiance is calculated using the following formula:

$$E_o = \frac{P_0}{A_d}$$

Where: P_o = measured power
A_d = area of the detection

6. Measure thickness of red filter with micrometer at two corners holding the filter by the edges. Record the average value in Data Table L2. Optical filters are delicate. Handle them with care. Ensure that the micrometer does not come in contact with a central portion of the filter. Do not get fingerprints on filter surfaces
7. Insert filter into filter holder. Carefully place filter in the path of the beam **near** the detector. Refer to Figure L2. Ensure that the reflected beam from the filter is directed back into the laser aperture.
8. Measure power (*P*) and record in Data Table L2.
9. Insert a second red filter into filter holder and record power (*P*) in Data Table L2. Assume thickness is

the same as the first filter. Range setting may need to be adjusted as transmitted irradiance drops. Do not adjust range below 100 μW. Power levels that cannot be read by the 100 μW range can be considered 0.

10. Repeat step 9 with up to six filters or where power drops to 0.
11. Calculate the irradiance and absorption coefficient (using the equation given in the introduction) and transmission, for each reading and thickness. Record in Data Table L2.
12. Repeat steps 6–11 with a set of blue filters and neutral-density filters.
13. Include in lab report a plot of transmission versus thickness for both red and neutral- density filters.

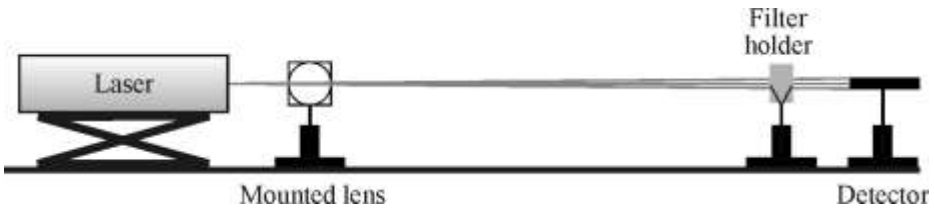

Figure L2 *Laser setup*

Data Table L1

Incident Beam	
Po (mW)	E_0(mW/cm^2)

Data Table L2

Red Filter				
x(cm)	P (mW)	E(mW/cm^2)	T(%)	Absorption Coefficient (cm^-1)
Blue Filter				
x(cm)	P (mW)	E(mW/cm^2)	T(%)	Absorption Coefficient (cm^-1)

ND Filter				
x(cm)	P (mW)	E(mW/cm^2)	T(%)	Absorption Coefficient (cm^-1)

Laboratory 2: To study the characteristics of image formed by a converging lens

The word *lens* comes from the Latin word for lentil, a seed whose shape is similar to that of a common lens. An optical lens is made from some transparent material, most commonly glass. One or both surfaces usually have a spherical contour. If both spherical surfaces are convex (bulge outwards), the lens is called the *biconvex* or *converging lens* (also called a *positive lens*). The properties of lenses are due to refraction of light passing through them. When light rays pass through a lens, they are refracted, or deviated from their original paths, according to the law of refraction.

A biconvex lens is a converging lens. Incident light rays parallel to the optic axis of the lens converge at a focal point on the opposite side of the lens. When light travels inside a lens, it is refracted and displaced laterally. A lens with spherical geometry has for each lens surface a center of curvature, a radius of curvature, a focal point, and a focal length. The focal points are at equal distances on either side of a thin lens. Opposite sides of a lens are generally distinguished as the *object side* and the *image side*.

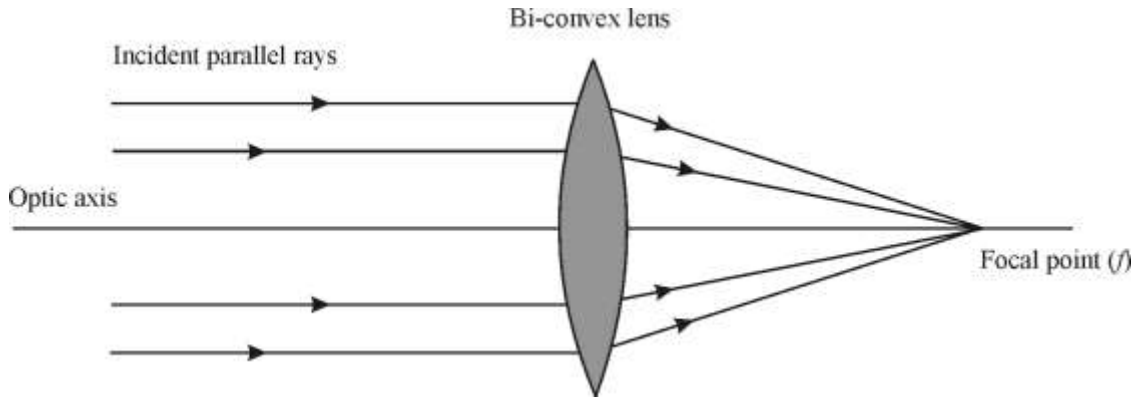

Figure L3 *Rays converging at the focal point (f)*

For a lens, the image of an object is *real* when formed or projected on the side of the lens opposite the object's location (on the image side) and *virtual* when formed on the same side of the lens as the object's location (on the object side). The characteristics of the image formed by a converging lens depend on the distance of the object in front of the lens. For a convex lens, the object is located within one of the three regions defined by the focal point f and twice the focal point $2f$ or at one of these two points, as shown in Figure L4.

If p is the object distance from the lens, for $p > 2f$, the image is real, inverted, and reduced. For $2f > p > f$, the image will also be real and inverted but enlarged or magnified. For $p < f$, the image will be virtual, upright, and enlarged. For $p = f$, the image forms at infinity. For $p = 2f$, the image is real, inverted, and the same size as the object. Figure L4 shows the image characteristics formed by a convex lens with respect to various object distances from the lens.

The image distances and image characteristics for a lens can be found analytically. The **thin- lens equation** (lens thickness is much smaller than the focal length) is

$$1/p + 1/q = 1/f$$

or

$$f = pq/(p+ q)$$

The magnification is:

$$M = -q/p$$

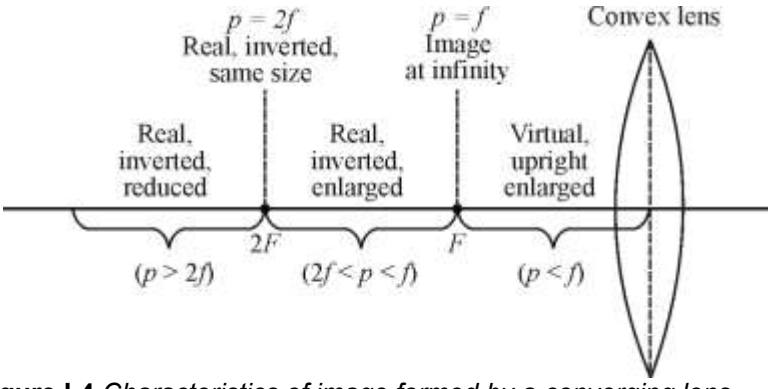

Figure L4 *Characteristics of image formed by a converging lens*

Objective

To find the focal length of a converging lens and describe image characteristics in each of three cases:

Case 1: $2f > p > f$

Case 2: $p = 2f$

Case 3: $p > 2f$

Equipment

Ruler
Scree
n
Light source with pattern (object)
Lens/screen holders
Three lenses of known focal length
Optical bench

Procedure

The experimental arrangement is shown in Figure L5. Use the following procedure in the sequence shown.

1. Measure the height of the object (vertical arrow) and record in Data Table L3.
2. Place the lens in the lens holder.
3. Check to make sure the optic axis is aligned straight.
4. Check to make sure the object is illuminated by the light source and remains fixed in position at one end of the measurement bench as shown.
5. The object distance *p* is the distance between the object and the lens.
6. The image distance *q* is the distance between the lens and the screen.
7. Choose the object distance $p = f$ and obtain a sharp image of the object on the screen. Record *p* in Table 1.

8. Measure the image in the vertical direction and calculate $M_{measured}$.
9. Use the object and image distance to solve for the experimental focal length. Record in Table 1.
10. Repeat steps 1 through 7 for object distance equal to 2*f* and for an object distance greater than 2*f*.
11. Repeat this procedure for the next two lenses provided to obtain *p* and *q* experimentally.
12. Find magnification *M* and describe image characteristics.
13. Calculate the *percent error* between measured and the actual values of *f* using, % error = (f_{actual} – f_{exp})/f_{actual}.
14. Record observations and data in Table 1.

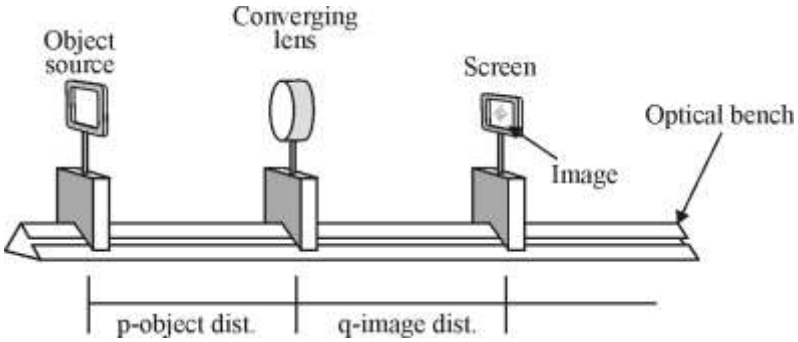

Figure L5 *Arrangement for measuring image characteristics using a converging lens*

Data Table L3

f_{actual} (cm)	f_{meas} (cm)	*p* (cm)	*q* (cm)	*h*' (cm)	M_{meas}= *h*'/*h*	*M*actual= –*q*/*p*	Image characteristics *f* % error
10	9.76	15	28	4.5	–1.5	–1.86	Magnified, inverted, real 2.4
10							
10							
15							
15							
15							
20							
20							
20							

Object height (*h*) =_____(cm)

Equations

$$f = \frac{qp}{q+p};$$

$$M = -\frac{q}{p}$$

$$M_{measure} = \frac{object\ high}{image\ hight}$$

Bibliography

Fried NM. Lectures from Introduction to Physics in Medicine, Department of Physics and Optical Science, University of North Carolina at Charlotte, 2020.

Fried NM. Lectures from Introduction to Biomedical Optics, Department of Physics and Optical Science, University of North Carolina at Charlotte, 2021.

Izatt JA. Optical Coherence Tomography, SPIE course.

Kane SA and Gelman BA. Introduction to Physics in Modern Medicine, CRC press, 2020.

Keiser G. Biophotonics: Concepts to Applications, Springer, 2016.

Wang LV and Wu HI. Biomedical Optics. Wiley, 2007.

Glossary

(listed in Alphabetical Order)

A-scan: An “amplitude” scan, consisting of a single line of reflection intensity data in the depthwise or axial direction, along the optical axis.

Attenuation: The loss of light through either absorption and/or scattering.

Axial resolution: The ability to distinguish between two close objects in the depthwise direction, along the direction that the light travels.

Ballistic photons: The photons travel in a straight line through the tissue, like a bullet, with no change in direction and minimal or no scattering.

B-scan: A “brightness” scan, consisting of a series of A-scans, allowing reconstruction of a two dimension image consisting of one depthwise and one lateral dimension.

Buffer: The outermost layer of an optical fiber, also sometimes referred to as the jacket, which provides protection and mechanical support for glass fibers under ending conditions, as well as insulation from the surrounding environment. The layer is commonly made of a polymer material.

Chromophore: A part of a molecule that absorbs light at a specific wavelength and is responsible for its color.

Cladding: The outer layer of an optical fiber that reflects light during total internal reflection.

Coherence: A property of light when the photons travel in phase.

Coherence length: The propagation distance over which a coherent wave maintains a specified degree of coherence.

Confocal parameter: Twice the distance of the Rayleigh length.

Continuous-wave: The property in which light is emitted continuously without interruption.

Core: The innermost layer of an optical fiber in which the light travels.

Cornea: A transparent layer forming front of the eye, which also acts as the outermost lens for focusing light

Critical angle: Light rays traveling at a greater angle than the critical angle will be totally internally reflected, while light rays traveling at a lesser angle will be refracted through the interface.

C-scan: A two dimensional image consisting of both lateral dimensions, at which the depth is fixed, also referred to as *en face* imaging.

Depth of focus: The distance between the two extreme axial points behind a lens at which an object is judged to be in focus.

Diffuse photons: These photons undergo multiple scattering events within the tissue, and take an indirect path through the tissue.

Diffraction: Interference of light waves passing through a narrow aperture or edge.

Distal: The far end or output end of a system, for example of an optical fiber or endoscope.

Doppler shift: The change in frequency of a wave from a moving source in relation to an observer.

Endoscope: A telescope used to see inside a natural opening in the body.

Epifluorescence: The fluorescence in an optical microscope when irradiated from the viewing side.

Epithelium: A cell layer that covers the outer surface of a tissue.

F number: The ratio of an optical element's focal length to the diameter of its clear aperture.

Fluorophore: A component of a molecule which allows it to fluoresce or emite light of a different wavelength than the excitation wavelength.

Fluoroscopy: A medical imaging technique that uses continuous x-rays, or an x-ray movie, to track motion within the body, for example the insertion of medical instruments such as catheters with radiopaque markers.

Focus: a point where light rays originating from a point on the object converge

Gaussian: A bell shaped curve.

Hemoglobin: A red protein responsible for transporting oxygen in the blood.

Image brightness: The overall lightness or darkness of an image.

Image contrast: The ability to distinguish between differences in intensity between an object and its surroundings, which can be quantified as a signal-to-noise ratio.

Immunofluorescence: The use of fluorescent dyes to label antibodies or antigens.

Irradiance: The power density.

Lateral resolution: The ability to distinguish between two close objects in the lateral direction, perpendicular to the direction that the light is traveling, or in the transverse direction.

Magnification: The size of an image relative to the size of the object creating the image, given by the ratio of the image length to the object length.

Mean free path: The distance that a photon is likely to travel before being either absorbed or scattered.

Melanin: A dark brown or black pigment found in hair, skin, and the iris of the eye. It is responsible for the tanning of skin exposed to sunlight.

Monochromatic: Light that has a single narrow wavelength.

Multimode: For an optical fiber, multiple or many modes of light propagation, or different paths, are supported by the fiber core.

Near-infrared spectrum: Part of the electromagnetic spectrum referring to light with wavelengths greater than 700 nm, but less than approximately 3000 nm, as defined by the medical field.

Numerical aperture: Sine of the half angle for light either entering or leaving an optical element (e.g. a lens or optical fiber).

Optical penetration depth: The depth at which light penetrates a tissue before being attenuated or lost (due to absorption and scattering), where the irradiance decays to 1/e or 37% of its initial value at the tissue surface.

Photobleaching: The process in which excessive exposure of light intensity on a fluorophore destroys its absorption and emission properties. In other words, loss of color by a pigment under illumination,

Polychromatic: Light that consists of a broad band of multiple wavelengths.

Protein: A large molecule that is an essential structural component of tissues.

Q-switched: Delivery of light in short pulses on the order of nanoseconds.

Quantum yield: a measure of the efficiency of photon emission, given by the ratio of the number of photons emitted to the number of photons absorbed.

Raman scattering: An inelastic scattering process, in which there is an exchange of energy, such that the emitted light has a different wavelength and direction than the absorbed light.

Rayleigh length: The distance from the beam waist at which the beam radius is increased by a factor of the square root of two.

Rayleigh scattering: The scattering of light by particles in a medium, without a change in wavelength, otherwise referred to as elastic scattering.

Reduced scattering coefficient: This parameters takes into account the directional scattering or anisotropy factor, g, in providing a more accurate representation of the effects of light scattering.

Refractive index: The ratio of the speed of light in vacuum divided by the speed of light in a medium.

Resolution: The smallest scale at which two close objects can be seen as separate

Retina: A layer at the back of the eye containing cells that are sensitive to light and that trigger nerve impulses that pass via the optic nerve to the brain, where a visual image is formed.

Scattering coefficient: A measure of how strongly tissue scatters light.

Single mode: For an optical fiber, only one mode of light propagation, or path, is supported by the fiber core.

Snake photons: These photons undergo multiple scattering events, but are highly scattered in the forward direction, also referred to as quasi-diffuse photons.

Spatial beam profile: The shape or structure of the laser beam, providing information on how the energy is distributed in space across the laser spot.

Stokes shift: The difference in wavelength at which a molecule emits light relative to the wavelength at which it is excited.

Tomography: A technique used to show a single plane, or slice, of an object.

Total attenuation coefficient: This parameter takes into account both the absorption and scattering coefficients.

Total internal reflection: The process of light traveling down the core of an optical fiber and being reflected multiple times at the core/cladding interface.

Credits for Graphics

Figure 1. Adapted from H. M. Subhash and R. Wang, “Optical coherence tomography: technical aspects,” 2013.

Figure 2. Courtesy of:

(a) Adison Wesley Longman, inc.

(b) Enchantedlearning.com

Figure 3. Courtesy of www.schoolphysics.co.uk

Figure 4. Courtesy of S. T. Ross, J. R. Allen, and M. W. Davidson, “Practical considerations of objective lenses for application in cell biology,” Methods in Cell Biology 123:19-34, 2014.

Figure 5. Courtesy of: M. W. Davidson, Florida State University, Molecular Expressions Optical Microscopy Primer website.

Figure 6. Courtesy of Leica Microsystems, inc. (Buffalo, Grove, IL)

Figure 7. Same figure as 1st edition.

Figure 8. Same figure as 1st edition.

Figure 9. Courtesy of S. Shah, J. Yang, J. Crawshaw, O. Gharbi, and E. Boek, Edo, “Predicting porosity and permeability of carbonate rocks from core-scale to pore-scale using medical CT, confocal laser scanning microscopy, and micro CT,” Proceedings - SPE Annual Technical Conference and Exhibition, 2013.

Figure 10. Adapted from Nathaniel Fried’s lecture notes in Biomedical Optics course.

Figure 11. Courtesy of:

(a,b) S. Lopez, “Pulse oximeter fundamentals and design,” NXP Applications Notes, 2012.

(c) G. A. Diddy, S. L. Clark, and C. A. Loucks, Intrapartum fetal pulse oximetry: past, present, and future," American Journal of Obstetrics and Gynecology 175(1):1-9, 1996.

Figure 12. Same figure as 1st edition.

Figure 13. Courtesy of:

(a) Pavlina

(b) Edinburgh Instruments (United Kingdom)

Figure 14. Courtesy of:

(a) Sprawls.org

(b) Adapted from S. A. Kane and B. A. Gelman, Introduction to Physics in Modern Medicine, 3rd Ed, CRC press, 2020.

Figure 15. Courtesy of D. Fried, "Detecting dental decay with infrared light," Optics and Photonics News, pp. 48-53, May 2020.

Figure 16. Courtesy of D. Fried, "Detecting dental decay with infrared light," Optics and Photonics News, pp. 48-53, May 2020.

Figure 17. Courtesy of computertomography.weebly.com. Inset from 1st edition.

Figure 18. Courtesy of G. Krishnamurthy, "Positron emission tomography: function and uses," Stanford University, 2015.

Figure 19. Courtesy of Hong Kong Association of Medical Physics website.

Figure 20. Courtesy of:

(a,b) Ekta's Physics E-Portfolio website

(c) minjikim-md.tistory.com

Figure 21. (a, b) Adapted from Nathaniel Fried's lecture notes from Introduction to Physics in Medicine course.

Figure 22. Courtesy of course on ultrasound at Washington University, Saint Louis, MO. (courses. washington.edu)

Figure 23. Courtesy of www.radiologycafe.com

Figure 24. Courtesy of the International Society for Optics and Photonics (SPIE) course on Optical Coherence Tomography, Joseph Izatt.

Figure 25. Adapted from Nathaniel Fried's lecture notes in Biomedical Optics course.

Figure 26. Courtesy of NKT Photonics website (Denmark).

Figure 27. Courtesy of the International Society for Optics and Photonics (SPIE) course on Optical Coherence Tomography, Joseph Izatt.

Figure 28. Courtesy of Bob Mellish (United Kingdom)

Figure 29. Courtesy of W. Drexler, Y. Chen, A. D. Aguirre, B. Povazay, A. Unterhuber, and J. G. Fujimoto, "Ultrahigh resolution optical coherence tomography," Optical Coherence Tomography, pp. 277-318, Springer, 2015.

Figure 30. Courtesy of the International Society for Optics and Photonics (SPIE) course on Optical Coherence Tomography, Joseph Izatt.

Figure 31. Courtesy of the International Society for Optics and Photonics (SPIE) course on Optical Coherence Tomography, Joseph Izatt.

Figure 32. Adapted from Nathaniel Fried's lecture notes in Biomedical Optics course.

Figure 33. Courtesy of:

(a) Nathaniel Fried's lectures on Biomedical Optics.

(b) G. Taubes, "Play of light opens a new window in the body," Science 276:1991-1993, 1997.

Figure 34. Courtesy of:

(a) Y. Yamada and S. Okawa, “Tomography: present status and its future,” Optical Review 21(3): 185-205, 2014.

(b) “New era scanning technology – optical brain scanner with diffuse optical tomography technology (Dot) talkknowledge.blogspot.com

Figure 35. Courtesy of Y. Yamada and S. Okawa, “Tomography: present status and its future,” Optical Review 21(3): 185-205, 2014.

Figure 36. Courtesy of A. R. Mohammadi-Nejad, M. Mahmoudzadeh, M. Hassanpour, F. Wallois, O. Muzik, C. Papadelis, A. Hansen, H. Soltanian-Zadeh, J. Gelovani, and M. Nasiriavanaki, “Neonatal brain resting-state functional connectivity imaging modalities,” Photoacoustics 10:1-19, 2018.

Figure 37. Courtesy of J. Yao and L. H. Wang, “Eavesdropping on oxygen metabolism, SPIE newsroom, July 2012.

Figure 38. Courtesy of X. Wang, Y. Pang, G. Ku, X. Xie, G. Stoica, L. V. Wang, Lihong, “Noninvasive laser-induced photoacoustic tomography for structural and functional in vivo imaging of the brain,” Nature Biotechnology. 21:803-806, 2003.

This page was intentionally left blank